C.1

THE ALKALINE SULPHIDE LEACHING OF TETRAHEDRITE CONCENTRATE

by

REIN RAUDSEPP

B.Sc., (Engineering Chemistry), Queen's University, Kingston, Ontario, 1975

A THESIS IN PARTIAL FULFILMENT OF
THE REQUIREMENTS FOR THE DEGREE OF
MASTER OF APPLIED SCIENCE

in

THE FACULTY OF GRADUATE STUDIES
Department of Metallurgical Engineering

We accept this thesis as conforming
to the required standard

THE UNIVERSITY OF BRITISH COLUMBIA

March 1981

In presenting this thesis in partial fulfilment of the requirements for an advanced degree at the University of British Columbia, I agree that the Library shall make it freely available for reference and study. I further agree that permission for extensive copying of this thesis for scholarly purposes may be granted by the Head of my department or by his or her representatives. It is understood that copying or publication of this thesis for financial gain shall not be allowed without my written permission.

Rein Raudsepp

Department of Metallurgical Engineering
The University of British Columbia
2075 Westbrook Mall
Vancouver, B.C.
Canada
V6T 1W5

Date Mar. 5, 1981

Abstract

An investigation was made into the leaching of tetrahedrite concentrate by strong sodium sulphide/sodium hydroxide solutions. The experiments were designed to avoid oxidation of the elements present and so, solubilize antimony as antimony (III) - sulphide complexes. Analytical techniques were developed for the analysis of caustic and sulphur species (S^{2-}, S^{o}_{x-1}, $S_2O_3^{2-}$ and SO_3^{2-}) in antimony-containing solutions.

The quantity of antimony extracted from the tetrahedrite was found to be a function of both the sulphide and hydroxide concentrations. Sodium thioferrate, a reaction product of pyrite and sodium sulphide, was indicated as a leaching agent. The solid concentrate decomposition product was x-ray amorphous and colloidal. Though a positive identification of this material was not possible it was found that one iron and one sulphur were added to the product for each antimony extracted from the tetrahedrite.

An analysis of literature stibnite solubility data was done and showed that below log [Sb] (M) = -0.7 . $Sb_2S_4^{2-}$ is probably the predominant antimony (III) - sulphide complex in saturated soltuion at 25°C. Above log [Sb] (M) = -0.7 , $Sb_4S_7^{2-}$ is the most likely predominant complex.

The results of the leaching study are not directly applicable to commercial tetrahedrite leach processes where the solutions contain oxidized sulphur species, in particular polysulphide. Antimony leached in these processes exists as antimony (V) - sulphide complexes.

Table of Contents

List of Tables

List of Figures

ACKNOWLEDGEMENTS

I would like to sincerely thank my supervisor, Dr. E. Peters, for the many, many hours he spent with me in consultation on this project. I would also like to thank all the members of the Metallurgy Department for their unending assistance and support.

I am grateful to the Sunshine Mining Co. for supplying the tetrahedrite concentrate used is this study. The financial support of the National Science and Engineering Council is greatly appreciated.

Chapter 1.

Introduction

1.1 General

Tetrahedrite is a copper antimony sulphosalt of widespread occurrence and of varied elemental substitution. Its primary metallic constituent is copper, but economically significant quantities of silver are often associated with this mineral.

Antimony (along with arsenic, the major substituent for antimony in tetrahedrite) is difficult to separate from copper by conventional reverberatory furnace-converter copper pyrometallurgy. That portion which is separated is largely volatilized during converting and must be removed from a sulphur dioxide-laden gas stream to avoid environmental contamination. Antimony and arsenic are also volatilized by matte smelting. The small amounts of these two elements which report to the blister copper dissolve during electrorefining and remain in the tankhouse electrolyte solution from which they must be purged or stripped. For these reasons significant economic penalties are assessed against the antimony and arsenic content of concentrates by custom copper smelters.

Antimony is soluble in sulphide solution (as is arsenic) and leaching processes for stibnite, Sb_2S_3, apply this

chemistry. Similar lixiviants can extract antimony from tetrahedrite leaving solids suitable for copper smelting. A plant based on this leach has operated in Sunshine, Idaho since 1942. Another plant under construction in Houston, British Columbia is expected to begin operation in 1981.

The purpose of this study was to investigate the equilibrium between tetrahedrite and sodium sulphide/sodium hydroxide leach solutions, and to determine the nature of the leach products. Industrial leaching processes are operated to produce the highest practical metal concentration in solution, and so this work was focused on equilibrium experiments done in strong solutions. A leach temperature of 100°C was chosen to conform with industrial practice, and Sunshine concentrate (which contains minerals other than tetrahedrite) was leached. The results obtained are not directly applicable to the Sunshine process since the Sunshine leach solution contains oxidized sulphur species not considered in this work. These species, polysulphide and thiosulphate in particular, are potential oxidants in the leaching chemistry.

1.2 Tetrahedrite

Sulphosalts are a class of minerals which have the general formula $A_m T_n X_p$ where the elements designated as A are: Cu, Pb, Ag; as T: As, Sb, Bi and as X: S (Takeuchi and Sadanaga, 1962). Within their structure there is a trivalent T species covalently bonded to three sulphurs to form a low pyramid with T at the vertex. The presence of these anionic TS_3 pyramids, arranged either singly or in complex groups, distinguishes sulphosalts from sulphides.

Tetrahedrite, a copper antimony sulphosalt, has the nominal formula $Cu_{12}Sb_4S_{13}$. Its crystal structure was originally believed to be derived by an orderly substitution of sphalerite, ZnS, which has tetrahedra of zinc and sulphur about each other. However, the inability of antimony to form a fourth bond produces distortions and sulphur vacancies relative to the sphalerite lattice. In tetrahedrite half the copper atoms are tetrahedrally bonded to four sulphurs, while the other half are trigonally coordinated to three (Wuensch, 1964).

Above 95°C tetrahedrite shows a wide solid solution range: $Cu_{12+x}Sb_{4+y}S_{13}$, where $0.11 < X < 1.77$, $0.03 < Y < .30$ (Tatsuka and Morimoto, 1973). Below 95°C the solid solution readily dissociates into two immisible tetrahedrite phases: one copper-poor, the other copper-rich, with compositions approaching $Cu_{12}Sb_4S_{13}$ and $Cu_{14}Sb_4S_{13}$.

The copper atoms of tetrahedrite can diffuse rapidly and it

is possible to convert one form of tetrahedrite to the other by cold pressing with copper powder or sulphur (Tatsuka and Morimoto, 1973). Copper-poor tetrahedrite can be obtained by immersing the copper-rich phase into carbon disulphide containing 5% sulphur forming a copper sulphide (CuS) film.

With the partial substitution of copper and antimony by other elements only the copper-poor stoichiometry is found consistent with the compositions observed in natural tetrahedrites: $(Cu,Ag)_{10}(Fe,Zn,Hg,Cu^*)_2(Sb,As)_4S_{13}$ (Tatsuka and Morimoto, 1973). Cu* is limited to less than 0.2 atom in most natural specimens. Cu* has an upper limit of 0.8 when there is more than one Fe. The arsenic analogue of tetrahedrite is tennantite and the formula given above holds for both.

Iron is always found in tetrahedrite (1-13%) and zinc usually (0-8%); less commonly silver,lead and mercury substitute for copper. The argentiferous variety, known as freibergite, contains up to 18% silver (Hurlbut and Klein, 1977).

Tetrahedrite is usually found in hydrothermal veins of copper, silver, lead and zinc. It is often associated with chalcopyrite, pyrite, sphalerite, galena and various other silver, lead and copper minerals (Hurlbut and Klein, 1977).

1.3 Chemistry

1.3.1 Alkaline Sulphur Chemistry

Sulphate should be the product of sulphide oxidation at 100°C in alkaline solution on the basis of thermodynamic reasoning. The 100°C sulphur E-pH diagram is shown in Figure 1-1. However, for kinetic reasons SO_4^{2-} may form only at potentials up to 0.5 volt higher than those thermodynamically required. The sulphur oxidation state diagram at pH 12 (Figure 1-2) indicates that if the potential for SO_4^{2-} formation were to be raised, more significant concentrations of polysulphide, $S_2O_3^{2-}$ and SO_3^{2-} would exist in solution.

Sulphide oxidation to sulphate under alkaline conditions is observed with iodine, iodate, hypochlorite and hydrogen peroxide oxidants (Blasius et al. , 1968). The potential of a partially oxidized solution is not determined by the S^{2-}/SO_4^{2-} couple (which is quite irreversible), but rather by the sulphide/polysulphide couple (Ferreira, 1975). Though the equilibrium concentration of polysulphide is small in alkaline solution, a very reversible equlibration with sulphide occurs. When sodium sulphide, $Na_2S \cdot 9H_2O$, is dissolved in water, HS^- and OH^- are formed by hydrolysis (Equation 1-1).

$$nNa_2S + mNaOH + n(F-1)H_2O = nF\ Na_2S + n(F-1)NaHS + \{m + n(F-1)NaOH\} \quad ...(1-1)$$

Figure 1-3 shows the fraction of added Na_2S which exists as S^{2-} at 100°C as a function of the initial Na_2S and NaOH

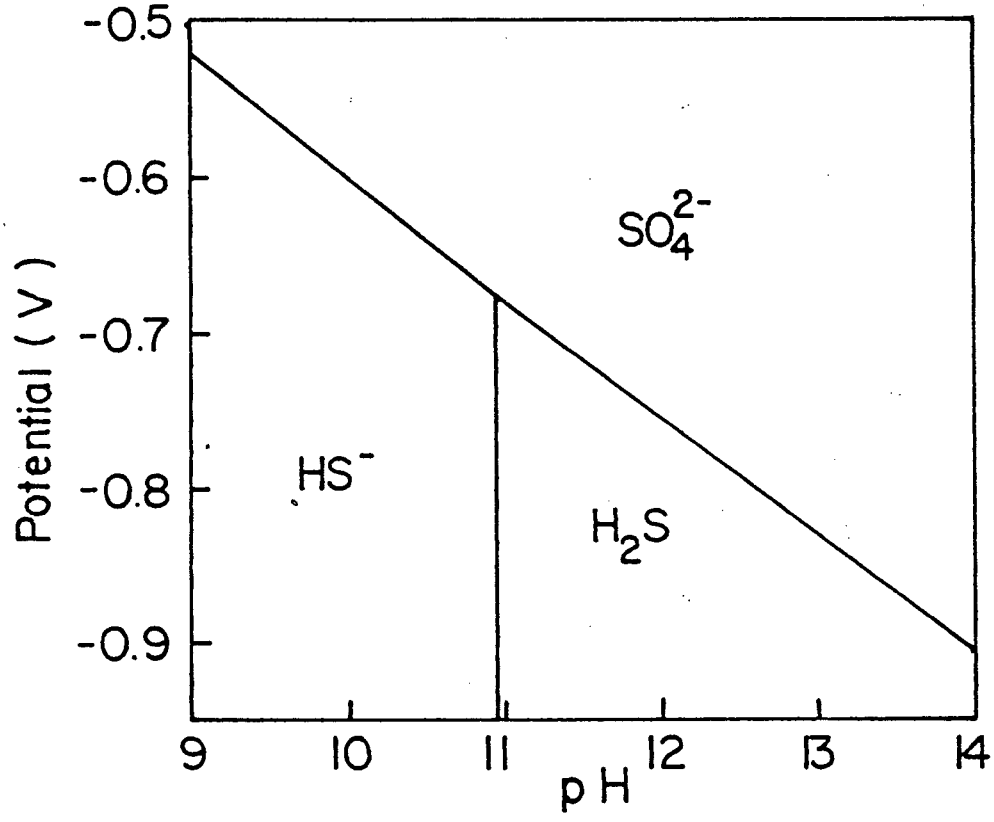

Figure 1-1: Sulphur E-pH Diagram at 100°C

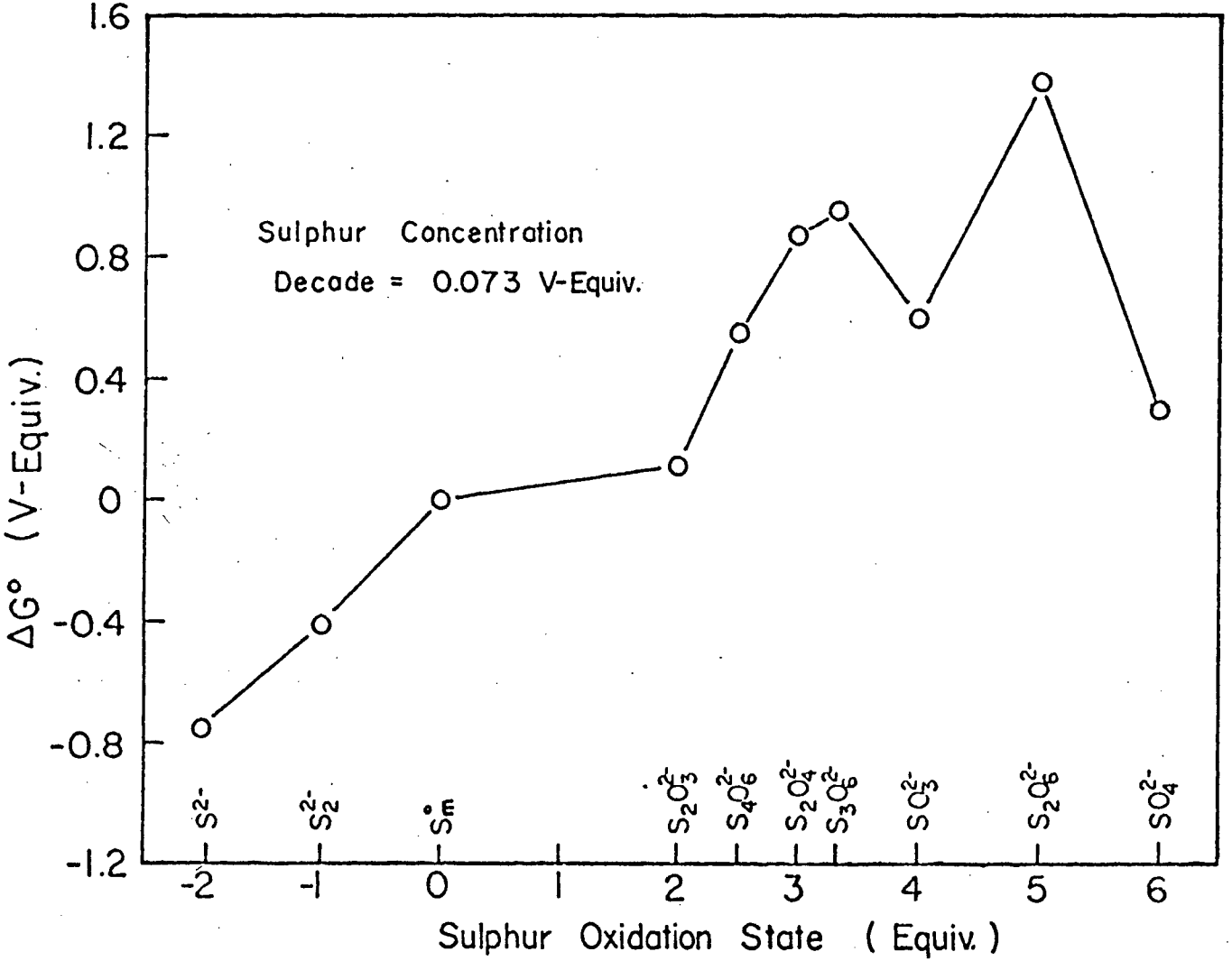

Figure 1-2: Sulphur Oxidation State Diagram at 100°C , pH=12

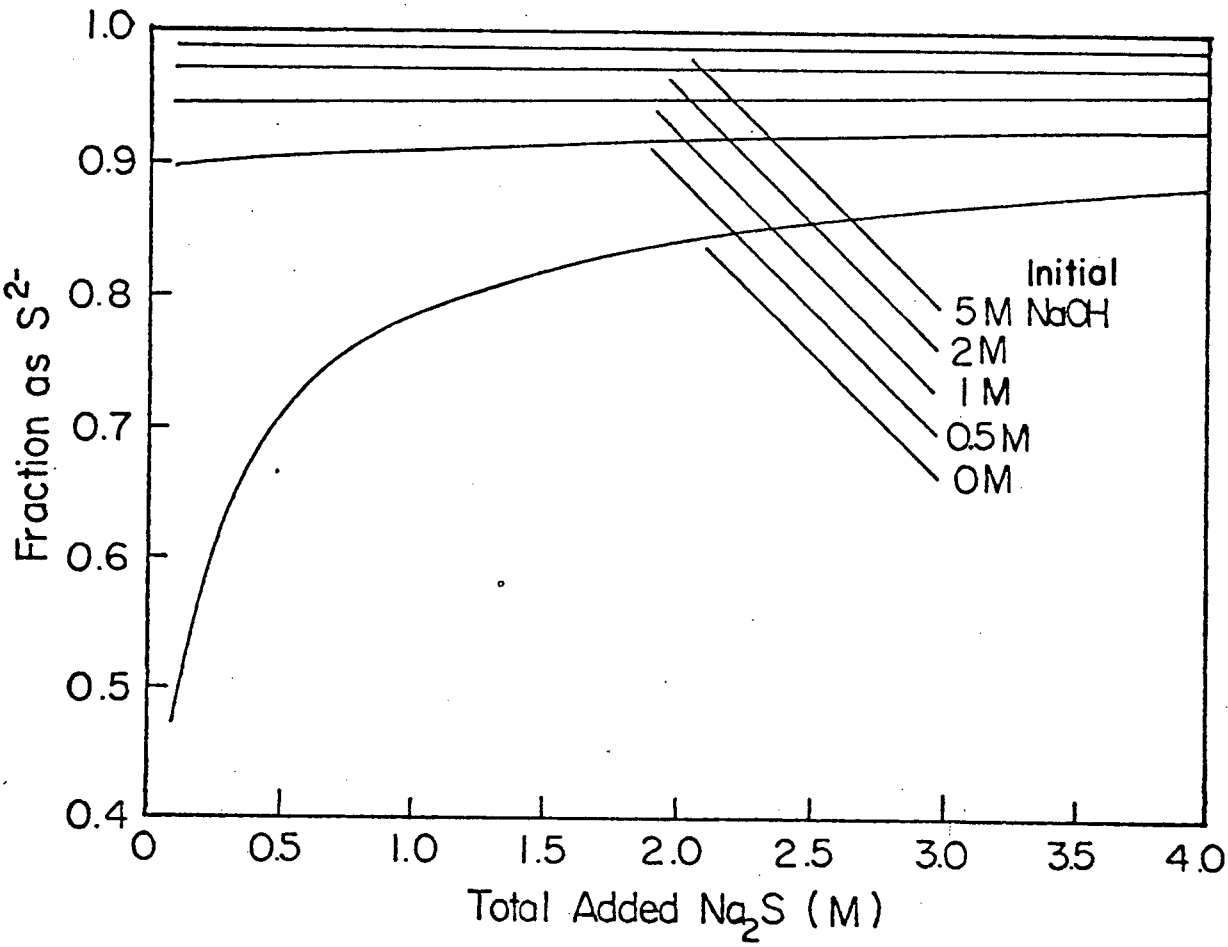

Figure 1-3 Fraction of Added Sodium Sulphide as the S^{2-} Ion at 100°C

concentrations. Appendix A shows the calculations used. Unit activity coefficients were assumed for all species as no activity data was available for HS^- and S^{2-}.

1.3.2 Alkaline Antimony-Sulphur Chemistry

Antimony has two major oxidized valence states, Sb (III) and Sb (V). Both form binary sulphur compounds and soluble sulphide complexes.

The Sb (III)-sulphur binary compound is stibnite, Sb_2S_3. In the stibnite structure (Scavnicar, 1960) half the antimony atoms are bonded to three sulphurs in a trigonal SbS_3 pyramid as in Sb sulphosalts. The other half is bonded to five sulphurs in a square S_5 pyramid. By a valence electron hybridization argument (Scavnicar, 1960) Sb(III) completes its 5 s^2p^3 valency shell to an octet of four tetrahedrally arranged electron pairs by forming three covalent bonds in trigonal pyramid configuration. If the two d electrons are considered in sp^3d^2 hybridization, the most probable configuration is six octagonally arranged electron pairs: a 5-coordinate pyramid plus a lone pair.

Complex sulphides with alkali metals have been prepared by high temperature salt fusion techniques (Moss and Smith, 1975). These salts are Na_3SbS_3, $Na_6Sb_4S_9$ and $NaSbS_2$ plus some of their Li, K, Rb and Cs analogues. They do not crystallize from aqueous solution. A comparison of the nuclear quadrapole

resonance spectra of Na_3SbS_3, $NaSbS_2$ and Ag_3SbS_3, a silver sulphosalt, indicated that the structures of the sodium salts were based on SbS trigonal pyramids (Buslaev et al. , 1971). The x-ray crystal structure of $K_2Sb_2S_7$ showed SbS_3 and Sb-centered S_5 groups (Moss and Smith, 1975).

Various Sb(III)-sulphide complexes have been proposed: SbS_2^-, SbS_3^{3-}, $Sb_2S_4^{2-}$, $Sb_2S_5^{4-}$ and $Sb_4S_7^{2-}$. However, their relative domains of stability have not been mapped out and it is not even certain that all of them exist. Some thermodynamic data and equilibria constants from stibnite solubility studies have been published (Table 1-1) (Sillen and Martell, 1964; Barner and Scheuerman, 1978; Butler, 1964; Latimer, 1952), but not all this information should be taken at face value. For example, Latimer's 1952 estimate of the ΔG° for SbS_3^{3-} remains unchanged in Barner and Scheuerman's 1978 compiliation of data despite a major change to Sb_2S_3's ΔG° which must have formed the basis for the original estimate. No activity coefficient data are available for any of the complexes.

Figure 1-4 shows possible structures for the Sb(III)-sulphides complexes listed above. SbS_2^- seems unlikely because there are no SbS_3 units. $Sb_2S_5^{4-}$ also seems unlikely because of the large number of singly bonded sulphurs. Covalently bonded sulphide is capable of two, four or six single bonds or four single and one double bond (Vaughan and Craig, 1978). The structure of $Sb_4S_7^{2-}$ shown is based on the stibnite unit cell (Scavnicar, 1960).

Table 1-1 : Proposed Stibnite and Antimony(III) Reactions*

$1/2\ Sb_2S_3\ (s) + 3/2S^{-2} = SbS_3^{-3}$	K(298) = 0.89
$1/2Sb_2S_3\ (s) + 1/2S_2^{-2} = SbS_2^{-2}$	K(298) = 0.45
$Sb_2S_3\ (s) + S^{-2} = Sb_2S_4^{-2}$	K(303) = 2.08
$Sb_2S_3 + HS^- = HSb_2S_4^-$ (?)	K(298) = -2.33
$SbS_2^- + S^{-2} = SbS_3^{-3}$	K(298) = 0.44

* References: Sillen and Martell (1964); Butler (1964)

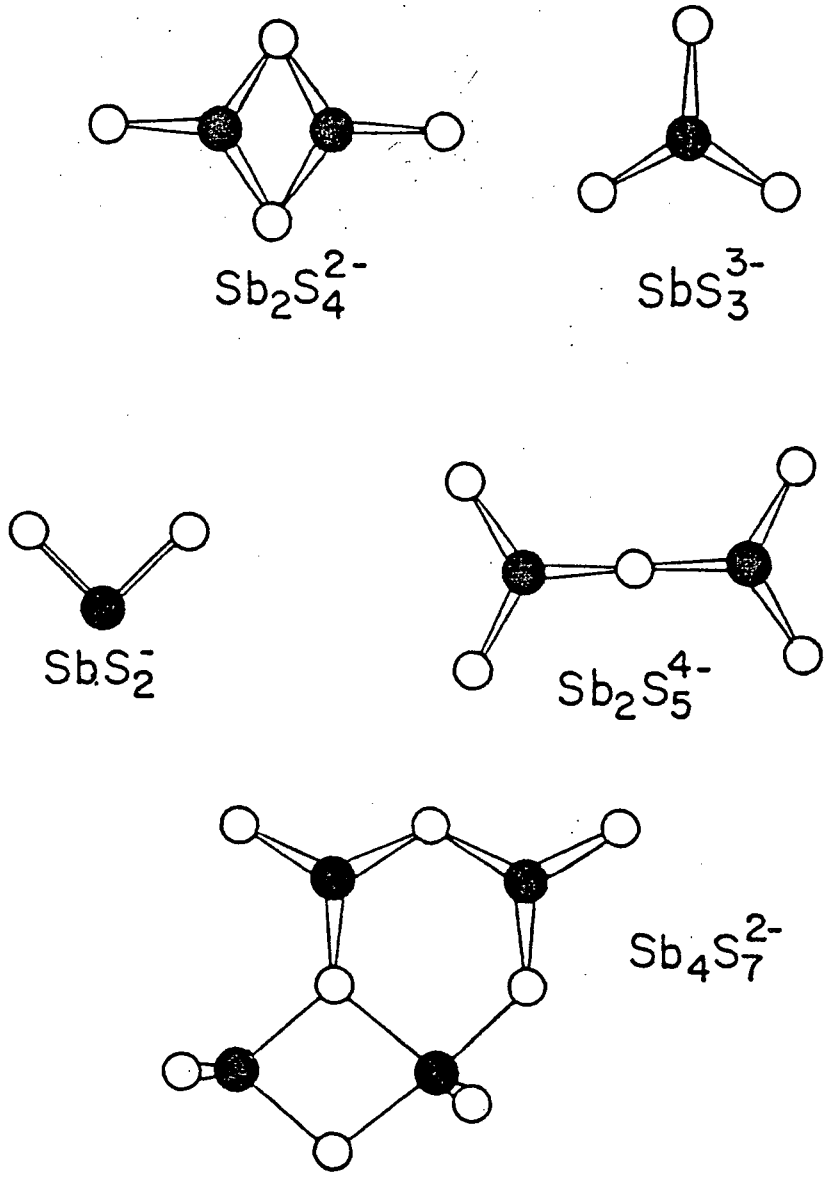

Figure 1-4: Structures for the Proposed Antimony(III)- Sulphide Complexes (Plan Views)

The simple aquated Sb^{3+} ion has never been detected (Moss and Smith, 1975) while antimony oxy-anions, SbO_2^- for example, are stable.

Antimony (V) sulphide, Sb_2S_5 (as precipitated), has been shown to contain only Sb(III) by Mossbauer spectroscopy (Moss and Smith, 1975). The only reported Sb(V)-sulphide aqueous complex is SbS_4^{3-}. Sodium thioantimonate, $Na_3SbS_4\ 9H_2O$, its solid analogue, can be crystallized from solution. The oxidation of Sb(III) to Sb(V) by polysulphide (Equation 1-2)

$$(x-1)SbS_3^{3-} + Sx^{2-} = (x-1)SbS_4^{3-} + S^{2-} \quad ...(1-2)$$

is reported to be quantitative (Sevryukov and Murti, 1966).

The electrolytic reduction of antimony sulphide complexes is the basis for industrial electrowinning. Various reduction potentials have been measured (Table 1-2).

1.3.3 Miscellaneous Alkaline Sulphide Chemistry

Many metal sulphides have extremely low solubility products and are considered to be virtually insoluble. However, metal concentrations in solution can be raised by many orders of magnitude if sulphide complexes are formed. Table 1-3 shows reactions which are possible in alkaline sulphide solution. Table 1-4 shows the measured solubilities of various metal sulphides and oxides in sulphide solution (presumably at 25°C). One reported solubility for copper from Cu_2S is given as 0.014 M in 1.1 M sulphide (Baiborodov *et al.*, 1975) whereas its

Table 1-2: Antimony-Sulphide Complex Reduction Potentials*

$SbS_2^- + 3e^- = Sb + 2S^{-2}$	$E^\circ = -0.85$ V
$SbS_3^{-3} + 3e^- = Sb + 3S^{-2}$	$E^\circ = -0.9$ V
$1/2\ Sb_2S_5^{-4} + 3e^- = Sb + 2.5S^{-2}$	$E^\circ = -0.86$ V
$SbS_4^{-3} + 5e^- = Sb + 4S^{-2}$	$E^\circ = -0.78$ V
$SbS_4^{-3} + 2e^- = SbS_3^{-3} + S^{-2}$	$E^\circ = -0.61$ V

*REFERENCES: Latimer (1952), Baibordov et al. (1975)

Table 1-3: Reactions Forming Soluble Sulphide Complexes*

	Log K(298)
$Ag^+ + S^{-2} = AgS^-$	23.9
$HgS(s) + S^{-2} = HgS_2^{-2}$	0.58
$As_2S_3(s) + 1/2\ S^{-2} = AsS_2$	1.0
$SnS_2(s) + S^{-2} = SnS_3^{-2}$	5.04
$2Au + 2HS^- + 1/2O_2(g) = 2AuS^- + H_2O$	29.7

*Rererences: Sillen and Martell (1964); Butler (1964)

Table 1-4: Solubility of Metal Sulphides and Oxides in Sodium Sulphide Solution*

	Metal Conc. (10^{-3} M)	Na_2S Conc. (M)
PbS	0.368	1.10
ZnS	0.384	1.10
CdS	0.1	1.10
FeS	1.96	1.40
Cu_2S	14.05	1.10
Cu_2S	1.8	1.45
MoS_2	9	1.40
Bi_2S	1	1.40
PbO	0.7	1.45
ZnO	5.5	1.53
CdO	1.9	1.45
Fe_2O_3	0.05	1.45
NiO	2.1	1.45

*Reference: Baibordov *et al.* (1975)

The solubility of sulphide minerals generally increases with temperature. Hydrothermal sulphide mineral deposits can be created by the localized precipitation of solid sulphides from hot natural waters by cooling (Vaughan and Craig, 1978).

Arsenic's sulphide solution chemistry is similar to that of antimony. A comparison of Tables 1-1 and 1-3 shows that AsS_2^- is 3.5 times more stable than its antimony analogue. In sulphide solution antimony is reduced from Sb(V) to Sb(III) in favour of As(III) oxidation to As(V) (Baiborodov, 1976).

The existence of ferric iron in sulphide solution as alkali metal thioferrate, $MFeS_2$, has recently been investigated (Taylor and Shoesmith, 1978). Thioferrate is reported to be a neutral colloidal species with a $(FeS_2)_n$ chain structure. The dispersed form was made by the addition of ferric ions to sulphide solution at pH 11-12. It had an intense green-black colour. The furthur addition of an equal volume of acetone, 1 M MOH or 1 M MCl flocculated a colloidal solid, $MFeS_2 \cdot x\ H_2O$ where M is Na or K. At 25°C both $NaFeS_2$ and $KFeS_2$ decomposed in acid solution (Equation 1-3).

$$2\ MFeS_2 + 6H^+ = 2M^+ + 2Fe^{2+} + 3H_2S + S^\circ \qquad ...(1\text{-}3)$$

At pH 11 and greater they were stable, but only with HS^- in solution. At 80°C $NaFeS_2$ decomposed rapidly even in the presence of HS^- (Equation 1-4) with the formation of polysulphide.

$$2NaFeS_2 = 2Na^+ + 2Fe^{2+} + S_2^{2-} + 2S^{2-} \qquad ...(1\text{-}4)$$

Lithium added as 1 M LiOH dispersed dry solid $NaFeS_2$ and $KFeS_2$

and ferric oxide/hydroxide was produced.

1.4 The Sunshine Leach Process

Leaching at the Sunshine plant (Barr, 1973; Holmes, 1944) is carried out on a batch basis in four 20 ton, covered, propeller agitated, steel tanks. Barren solution is pumped into a tank and heated by steam coils to begin the leaching cycle. When the solution reaches 95°C elemental sulphur and caustic solution are added to bring the Na_2S strength up to 300 g/l (3.8 M) and five tons of tetrahedrite concentrate are fed in. The leach goes for 14 hours at 100-103°C.

After leaching, the product slurry is pumped to a batch thickner and allowed to settle. The solids are filtered twice with water washing and shipped wet to a copper smelter. The filtration is difficult and the filter cake contains Na_2S and more than 20% moisture.

The clear pregnant solution is electrowon on mild steel cathodes producing a non-adherent depost: 95% Sb, 5% As, plus 6-10 oz/ton Ag. The anodes, also made of mild steel, are immersed in an anolyte solution which is separated from the catholyte by a canvas diaphragm. Both the catholyte and the anolyte are circulated about separate storage tanks until spent. The spent catholyte is used for leaching and to make up fresh anolyte which is 'de-sulphided' by anodic reactions. The spent anolyte is fully oxidized in an autoclave. The sodium antimonate

which is 'de-sulphided' by anodic reactions. The spent anolyte is fully oxidized in an autoclave. The sodium antimonate produced, $NaSb(OH)_6$, is settled out and releached while the liquid is sent to the concentrator tailings pond.

Since the leach solution is generated from caustic and elemental sulphur S^{2-}, $S_2O_3^{2-}$ and polysulphide, S_x^{2-}, are formed directly. (Equations 1-5 and 1-6)

$$4S^\circ + 6OH^- = 2S^{2-} + S_2O_3^{2-} + 3H_2O \quad ...(1-5)$$

$$(x-1)S^\circ + S^{2-} = S_x^{2-} \quad ...(1-6)$$

Oxidation produces sulphate. The leached antimony exists in the pentavalent form as SbS_4^{3-} due to the oxidizing power of polysulphide.

At the cathodes of the electrowinning cells the thioantimonate complex is reduced to metal (Equation 1-7).

$$SbS_4^{3-} + 5e^- = Sb + 4S^{2-} \quad ...(1-7)$$

The current efficiency of this process is lowered by the reduction of oxidized sulphur species, primarily polysulphide (Equation 1-8).

$$S_x^{2-} + 2(x-1)e^- = xS^{2-} \quad ..(1-8)$$

Sulphur oxidation reactions which consume sulphide and caustic take place at the anode (Equations 1-9 and 1-10, for example).

$$S^{2-} + 3OH^- = 1/2\ S_2O_3^{2-} + 3/2\ H_2O + 4e^- \quad ...(1-9)$$

$$1/2\ S_2O_3^{2-} + 5OH^- = SO_4^{2-} + 5/2\ H_2O + 4e^- \quad ...(1-10)$$

The anionic anodic products are kept away from the cathode by the diaphragm and electrostatic forces. The creation of

diaphragm adds to it as the OH^- ion has a relatively high transport number. Sodium ions migrate from the anolyte to the catholyte against the anions.

A partial mass balance about the Sunshine leach plant is given in Table 1-5.

Table 1-5: Sunshine Leach Plant Balance*

	Wt (%)	Cu (%)	Sb	Ag (OZ)	% Distribution Cu	Sb	Ag
In: Silver Conc	100	25.0	17.0%	1300	100	100	100
Out: Ag-Cu Residue	91	27.5	1.5%	1429	100	8.03	100
Sb Solution	8.1		70 g/l			81.97	
Discard Anolyte	0.9		10 g/l			10.00	

*Reference: Barr (1973)

Chapter 2.

Experimental

2.1 Materials

2.1.1 Tetrahedrite Concentrate

Tetrahedrite concentrate was received from the Sunshine Mining Co., Sunshine, Idaho. The material was passed through an 8-mesh screen to break up the lumps, mixed and bagged. The concentrate contained approximately 7.5% moisture and was used wet.

X-ray diffractometer results (shown in Appendix B) indicated the presence of tetrahedrite, argentian tetrahedrite, chalcopyrite, pyrite, marcasite and galena in the concentrate. Additional phases were undoubtedly present as represented by the unassigned lines, but the large total number of lines made their designation difficult.

X-ray fluorometry indicated the presence of antimony, copper, silver, arsenic, zinc and lead (only elements with an atomic number greater than 22 were detected by the instrument used). A partial chemical analysis of the concentrate is shown in Table 2-1. Table 2-2 shows wet screening results with a partial chemical analysis of each fraction. Antimony was

Table 2-1: Chemical Analysis of Sunshine Concentrate (Dry)

	%
Cu	26.0
Fe	14.6
Sb	13.1
S	29.1
As	1.58
Zn	1.67
Mn	0.19
Na	0.00
Ag	3.6*

*Analysis done by third year Metallurgy lab students.

Table 2-2: Wet Screening Results

Fraction (Mesh size)	% Retained	Analysis (%) Sb	Cu	Fe
+ 100	2.0	11.5	20.6	17.1
-100 + 140	5.7	11.1	20.8	19.1
-140 + 200	11.3	10.6	22.5	18.8
-200 + 270	13.6	10.2	24.2	17.3
-270 + 400	11.5	14.0	25.2	20.4
-400	52.7	13.6	27.8	13.4
Screen Loss	3.2			
Weighted Mean	(96.8%)	12.6	25.8	15.8

slightly more concentrated in the fine fractions.

A mounted and polished sample of concentrate was studied using the x-ray energy analyser of a scanning electron microscope (SEM). The tetrahedrite phase was found to contain iron, silver, zinc and arsenic as well as copper, antimony and sulphur. The commonly used sulphur and lead energy dispersed peaks virtually overlap, so small quantities of lead in tetrahedrite would be undetectable because of the large sulphur content. However, particles containing only lead and sulphur (galena) were found, as well as particles conforming with the phases determined in the diffractometer study. Particles containing silica, and iron, copper and manganese oxides were also found. The SEM x-ray analyser can detect elements with an atomic number greater than 9.

Based on the chemical and mineralogical analyses done, the concentrate can best be described as $(Cu_{9.7},Fe_{0.5},Zn_{0.8},Ag_{1.0})(Sb_{3.4}\ As_{0.6})S_{13}$ + 3.0 CuFeS + 4.6 FeS . The tetrahedrite composition indicated, $(Cu_{9.0}\ Ag_{1.0})$ $(Fe_{0.5},Zn_{0.8},Cu^{*}_{0.7})$ conforms with the observed compositions of natural tetrahedrites (Section 1.2). The concentrate composition calculation is shown in Appendix C.

A sample of the concentrate was leached with 1% HCl overnight in a sealed agitated flask at room temperature. A solution analysis by atomic absorption indicated that 10% of the concentrate's iron and 1% of its copper had been extracted. Iron and copper dissolved under these conditions will have been

present as oxides or salts, but not as sulphides.

2.1.2 Reagents

Reagent grade sodium hydroxide and sodium sulphide were used in the leaching studies. Deionized water was used throughout.

A 100 ml solution with 24.07 g of $Na_2S \cdot 9H_2O$ (1.002 M) was made up under anaerobic conditions. Analysis of the sulphur species gave 0.945 M S^{2-}, 0.041 M SO_3^{2-}, 0.024 M polysulphide sulphur (S°_{x-1}) and no $S_2O_3^{2-}$: 1.010 M total sulphur.(A sulphate analysis was not done.); similar solutions were assayed for their caustic content -these gave 0.019, 0.026, and 0.030 moles of caustic per mole sulphide.

2.2 Leaching Apparatus

The leach vessel was a round 150 ml pyrex flask with a flat bottom. The flask was sealed with a rubber bung through which a stirrer shaft passed encased in a 5 cm section of glass tubing. The stirrer was a triangular section of Teflon, approximately 1 cm per side, 2 cm long. This stirrer was easy to insert into the narrow-necked flasks and gave good mixing at 1400 rpm, the full speed of the Eberbach Lab-Stir motors used. These motors were unreliable when throttled to lower speeds and conventional stirrers were too violent at 1400 rpm.

The leach temperature was maintained by a violently boiling steam bath equipped with an automatic water level control set on a large Lindberg hotplate. Four leaching experiments could be accomodated simultaneously as shown in Figure 2-1. Each flask was clamped immersed to the neck with the concentric steam bath rings placed to keep the exposed boiling water surface area to a minimum.

The temperature of the leach mixture was measured to be 99.6°C. This steady state value was achieved five minutes after immersion of the flask into the bath.

2.3 Leach Procedure

Four leaching experiments were done simultaneously. The initial solutions were made up by dissolving solid reagents or by diluting stronger solutions. Care was taken to avoid sulphide oxidation. The sodium sulphide was dissolved in deaerated water in sealed flasks under nitrogen and only small well-sealed bottles of solid reagent were used to minimize oxidation during storage. Wet concentrate was weighed into the leaching flasks and pre-mixed solutions were added by pipette with a sample of each retained for analysis. The bungs and stirrers were inserted, the flasks clamped into the boiling water bath, and the agitation begun. The leaching time was 24 hours (± 15 minutes).

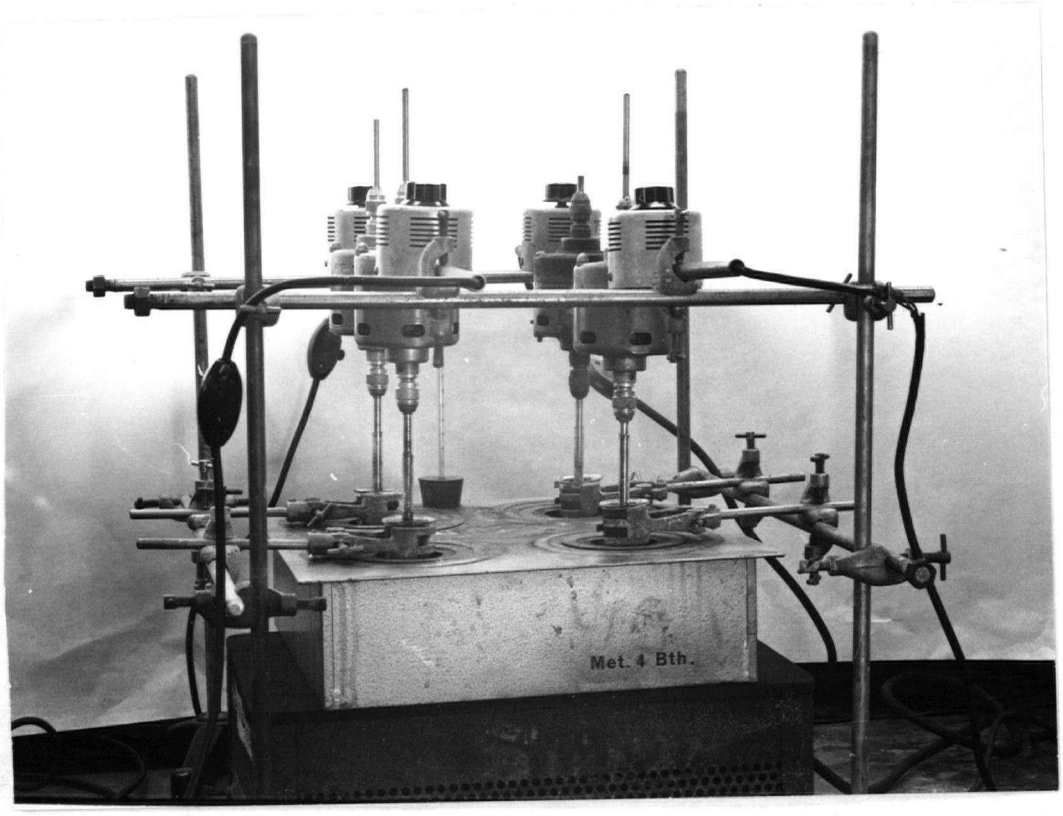

Figure 2-1 The Leaching Apparatus

The leach temperature of 100°C conformed with the industrial practice of the Sunshine Mining Co. leach plant, and was easy to maintain with a boiling water bath. Excess concentrate was used to achieve chemical equilibrium. An antimony extraction of less than 50% at equilibrium was the target. Twenty-four hours was considered to be an adequate time for the leach to equilibrate.

After leaching, the flasks were removed from the bath and a 15 ml slurry sample of each was taken and pressure filtered under N_2 through a fine glass frit. The bulk of each product slurry was dewatered and water washed on a Buchner funnel using pre-weighed fine filter paper (Whatman No. 42). The Buchner filtrates were made up to 500 ml and retained for analysis along with the pressure filtrates. The solution analyses were done immediately. The leach solids were dried, weighed and retained.

Before pressure filtration, the frits were pre-flushed with N_2. If this was not done, the first solution through would show the characteristic yellow colour of polysulphide.

The initial leach solutions were analysed for S^{2-}, $S_2O_3^{2-}$, and SO_3^{2-}. The final leach solutions were analysed for S^{2-}, S°_{x-1}, $S_2O_3^{2-}$, SO_3^{2-}, OH^-, Sb and As. The Buchner filtrates were analysed for Sb.

2.4 Sulphide Oxidation

To investigate sulphide oxidation, 85 ml per minute of air were bubbling through 500 ml of 0.855 M Na_2S after pretreatment with a 2 M NaOH solution. Both solution flasks were immersed in a boiling water bath. Over two hours of aeration no sulphide oxidation was observed in samples taken and analysed for S^{2-}, $S_2O_3^{2-}$ and S°_{x-1}. (This result was surprising as sulphide was expected to be more reactive.)

2.5 Evaporation

Evaporation was considered to be a problem because of the high vapour pressure of the water in the leach solutions at 100°C. Although the flasks were well sealed, the leach time was long. Evaporation was measured by weighing the leach flasks complete with their bungs and stirrers immediately before and after leaching experiments. Of 12 measurements taken, the average weight change of 11 was -0.32 g. (0.2% evaporation based on 130 ml of leach solution with 1 g of water per ml of solution.) the 12th. was -4.96 g (3.8% evaporation). Evaporation appeared to be a problem only in specific experiments rather than a general phenomenon.

Chapter 3.

Analytical Chemistry

3.1 Automatic Titration

The determination of caustic and sulphur species (S^{2-}, S°_{x-1}, $S_2O_3^{2-}$ and SO_3^{2-}) in the leach solution samples was done by automatic titration using a Radiometer RTS 822 titration system equipped with indicator and reference electrodes. The first derivative of the indicator-reference potential difference with respect to time was automatically plotted as a function of the titration volume. This derivative is effectively potential with respect to volume, $\Delta E/\Delta V$, since the titrations were done at a constant titrant addition rate.

The end point of a titration as defined by the maximum value of $\Delta E/\Delta V$ is identical with the true stoichiometric equivalence point only if the titration curve (potential as a function of volume) is symmetrical about the equivalence point (Bassett et al., 1978). A symmetric titration curve is produced when the indicator electrode is reversible and when there are an equal number of titrant reagent and reactant species in the equivalence equation. The pH titration curve for equation 3-1 would be symmetric; the potential titration curve for Equation 3-2 would not.

$$H^+ + OH^- = H_2O \qquad ...(3\text{-}1)$$

$$5Fe^{2+} + MnO_4^- + 8H^+ = 5Fe^{3+} + Mn^{2+} + 4H_2O \qquad ...(3\text{-}2)$$

The titration error, the difference between the end point and the equivalence point, is small when the potential change at the equivalence point is large (Bassett et al. , 1978). Most standard analytical titrations have a large equivalence point potential changes.

A titration error can also be generated if the solution contains a species which chemically interferes with the titrant or reactant and in doing so, distorts the titration curve symmetry. This error is greatest when the equilibrium constant for the reaction between the reactant (or the titrant) and an interfering species approaches the constant for the reaction between the titrant and the reactant. If the interference reaction is with the titrant, a second end point may be seen. In acid-base pH titrations an acid strength difference of six orders of magnitude (Δ pKa = 6) is required for the clean separation of two end points (Bassett et al. , 1978). The co-titration of OH^- (pKa = 14.0) and S^{2-} (pKa = 12.9) with acid shows only one end point. In all cases the magnitude of this type of titration error depends heavily on the relative quantities of the species involved.

As well as depending on solution chemistry factors, the accuracy of an automatically titrated end point also depends on the indicator electrode giving the correct potential for the titrant volume dispensed. The contents of the titration vessel have to be well mixed and the electrode must be in equilibrium

with the solution.

For the analytical titrations performed the most powerful stirrer available was used. In a test of the system a drop of dye was added to the titration vessel and was instantly dispersed. At the end point of each titration a slow rate was used, 0.05-0.20 ml per minute, to give the electrode time to achieve equilibrium. However, it is unlikely that equilibrium was ever completely achieved due to the rapid changes in potential at end points. Because of the slow rates used, the volume errors were not expected to be large.

The titration and first derivative curves for the titration of sodium sulphide with HCl are shown in Figure 3-1.

3.2 Soluble Sulphur Species Analysis

3.2.1 Sulphide, Polysulphide Sulphur, Thiosulphate And Sulphite Determination

The determination of S^{2-}, S°_{x-1}, $S_2O_3^{2-}$ and SO_3^{2-} was done by titration with $HgCl_2$ solution using a Radiometer RTS 822 titration system and Orion Ag/S specific ion and AgCl/Cl double junction reference electrodes. The method used was developed for the analysis of sulphur species in sulphide pulping liquors (Papp, 1971).

The active element of a Ag/S specific ion electrode is a

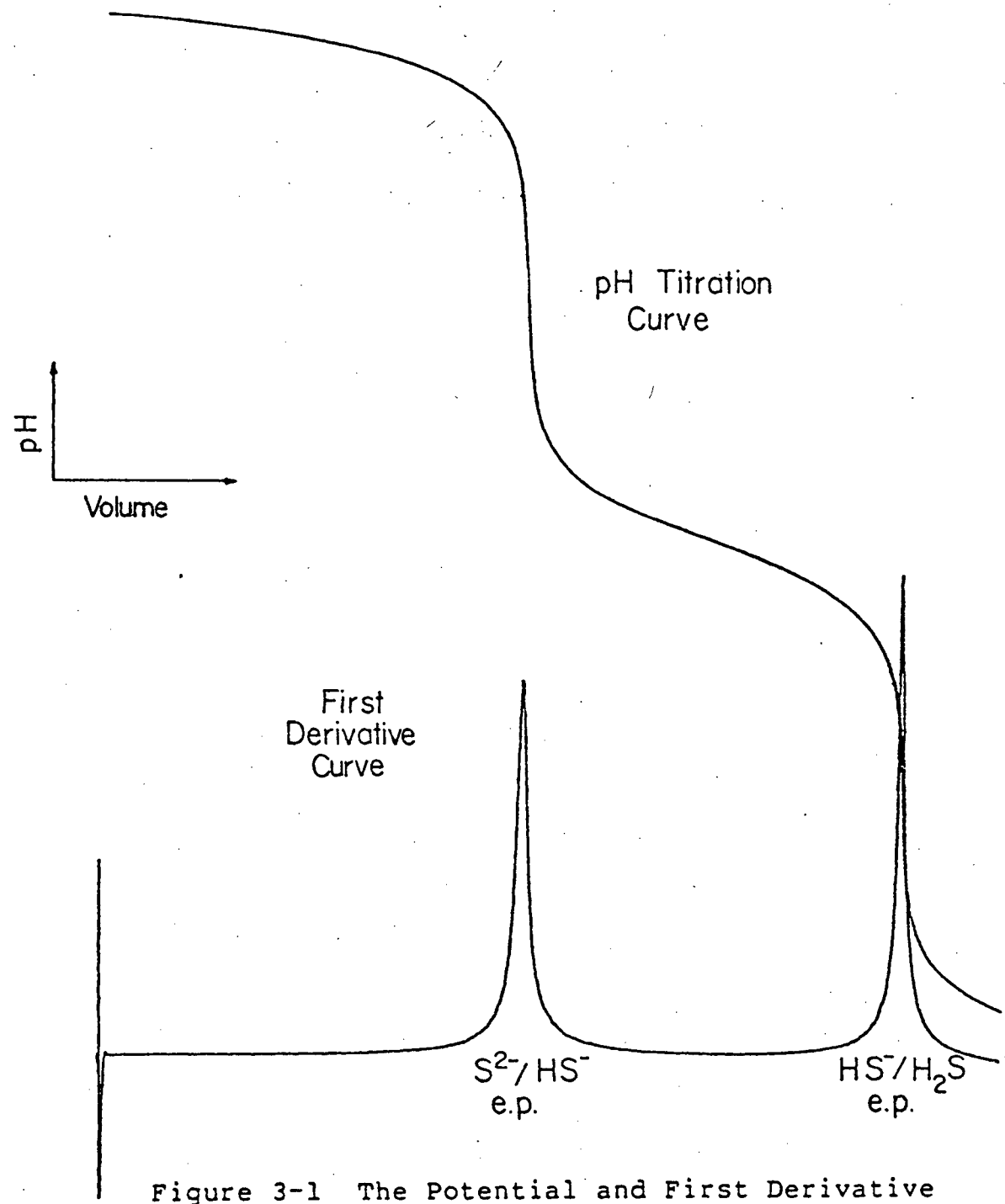

Figure 3-1 The Potential and First Derivative Curves for the Titration of Sodium Sulphide with Hydrochloric Acid

solid Ag_2S membrane which shows a Nerstian response to the activities of Ag^+ and S^{2-} over the activity range of of 10^{0} to 10^{-7} M in each. With mercuric ion in solution a HgS film forms on the membrane which must be occasionally removed. In sulphide solution the solution junction of a normal AgCl/Cl reference electrode would plug with precipitated Ag_2S. To avoid this, a double junction electrode is used with an outer filling solution of 10% KNO_3 made up to pH 12 with KOH.

When a mixture of sulphur anions: S^{2-}; S_x^{2-}; $S_2O_3^{2-}$; and SO_3^{2-}, is titrated with $HgCl_2$, S^{2-} reacts first (Equation 3-3), and the sulphide of S^{2-} next (Equation 3-4).

$$S^{2-} + Hg^{2+} = HgS \qquad ...(3-3)$$

$$S_x^{2-} + Hg^{2+} = HgS + (x-1)S^{\circ} \qquad ...(3-4)$$

Though it is possible to detect end points for free sulphide and for each polysulphide species (x = 2,3,...) the total sulphide is best determined on the basis of the final end point of the series which is unambiguous. Without extra caustic in solution the S^{2-} ion (the only sulphur ion that the Ag/S electrode responds to) is not stable enough to be determined independently of $S_2O_3^{2-}$ and SO_3^{2-}. The solution must be made up to 0.1-1.0 M NaOH.

After the sulphide end point the titration is stopped and the excess caustic is neutralized (pH 7.0-7.5) with 40% acetic acid. The titration is restarted and $S_2O_3^{2-}$ and SO_3^{2-} are determined together at the next end point (Equations 3-5 and 3-6).

$$S_2O_3^{2-} + Hg^{2+} = HgS_2O_3 \qquad ...(3-5)$$

$$SO_3^{2-} + Hg^{2+} = HgSO_3 \quad ...(3\text{-}6)$$

Although S^{2-} does not appear in these reactions, the electrode detects the excess Hg^{2+} present after the end point by the coupling of Hg^{2+} and S^{2-} in Equation 3-1. $S_2O_3^{2-}$ is determined by masking the SO_3^{2-} with formaldehyde (Equation 3-7).

$$HCHO + SO_3^{2-} + H^+ = CH_2OH\ SO_3^- \quad ...(3\text{-}7)$$

Polysulphide can be oxidized to $S_2O_3^{2-}$ by mild heating with Na_2SO_3 for 15 minutes (Equation 3-8).

$$S_x^{2-} + (x-1)SO_3^{2-} = S^{2-} + (x-1)S_2O_3^{2-} \quad ...(3\text{-}8)$$

The excess SO_3^{2-} is masked with formaldehyde and the incremental $S_2O_3^{2-}$ is reported as polysulphide sulphur, S°_{x-1}. A total sulphur species analysis requires three sets of determinations: S^{2-} and $S_2O_3^{2-} + SO_3^{2-}$; S^{2-} and $S_2O_3^{2-}$ (SO_3^{2-} by difference); and S^{2-} and S_2O_3 after Na_2SO_3 treatment (S°_{x-1} by difference).

The analytical procedure for a 1 M Na S solution containing small concentrations of the other sulphur species is as follows: A 5 ml sample is taken and made up to 100 ml. 5 ml aliquots of the diluted solution are pipetted into titration beakers with 2 ml of 10 M NaOH, and made up to 60 ml with deaerated water. The titrations are done immediately. Two microspatulas of reagent grade Na_2SO_3 are added to the beakers and the beakers are warmed on a hotplate over two asbestos pads for 15 minutes to oxidize the polysulphide. The $HgCl_2$ solution used in the analyses was 0.05 M which would give a S^{2-} titration of 5 ml for the sample described.

In practice the S^{2-} end point peaks of the derivative plots were large, sharp and easy to interpret. The $S_2O_3^{2-}$ and $S_2O_3^{2-}$

+ SO_3^{2-} peaks were smaller and broader but still easy to interpret if the volume separating them from the S^{2-} peak was greater than 0.2 ml. With smaller differences the peak structures were often complex suggesting interference effects. Small quantities of sulphide were always oxidized in the Na SO treatment. A reproducible end point, representing a very small titrant volume, was observed in some solutions immediately after the pH shift. Known additions showed that this peak was unaffected by $S_2O_3^{2-}$ or SO_3^{2-}. The prime suspect is considered to be polythionate, $S_xO_6^{2-}$ which has chemistry similar to S^{2-} and $S_2O_3^{2-}$ (Blausius et al. ,1968), but this was not confirmed. The titrant volume consumed by this species was subtracted where relevant.

3.2.2 The Effect Of Antimony(III) On The Sulphide Determination

To the author's knowledge, a $HgCl_2$ titration method for the determination of the sulphur species in antimony-containing solutions has not been reported.

Various quantities of technical grade stibnite were dissolved in Na_2S solution. Sulphide was determined by titration: antimony by atomic absorption analysis. The measured ratio of incremental S^{2-} to Sb was 1.60 ± 0.13 versus the stoichiometric ratio of 1.50 (Table 3-1). The determination of Sb(III)-complexed sulphide was considered to be quantitative.

Table 3-1: Sulphide Determination in Antimony(III) Solution

Sb_2S_3 Added (g/100ml)	Sb Calc. (g/l)	Sb Deter. (g/l)	S^{2-} (M)	$\Delta S^{2-} / \Delta Sb$ (mole/mole)
0			1.09	
0			1.08	1.09
0.57	4.09	4.16	1.15	1.78
1.06	7.60	7.44	1.18	1.52
1.53	11.0	10.8	1.21	1.43
2.00	14.3	14.2	1.26	1.53
2.62	18.8	18.6	1.34	1.64
3.12	22.4	22.1	1.40	1.72
			Mean =	1.60 ± 0.13 (95% C.L.)

3.2.3 The Effect Of Antimony(V) On The Sulphide And Polysulphide Determinations

Sodium thioantimonate, $Na_3SbS_4 \cdot 9H_2O$, was made by a procedure outlined by Sevryukov and Murti (1966). Various quantities of this salt were dissolved in deaerated water and S^{2-} and S°_{x-1} were determined by $HgCl_2$ titration while Sb was determined by atomic absorption analysis. The results are shown in Table 3-2.

Approximately four sulphides per antimony were determined in the sulphide analysis indicating a quantitative analysis for Sb(V)-complexed sulphide.

Sevryukov and Murti (1966) reported that the heating of Sb(V)-S^{2-} solutions with added Na_2SO_3 affected a reduction of the antimony (Equation 3-8).

$$SbS_4^{3-} + SO_3^{2-} = SbS_3^{3-} + S_2O_3^{2-} \qquad ...(3\text{-}8)$$

This would produce an apparent S°_{x-1} analysis and a drop in the S^{2-} analysis equivalent to the amount of Sb(V) present. The results show that the Sb to S^{2-} ratio dropped after the Na_2SO_3 treatment but did not reach three. The reduction reaction conditions were apparently inadequate to complete Equation 3-8. The incremental $S_2O_3^{2-}$ (S°_{x-1}) accounted for only about one-half of the drop in sulphide.

A drop in S^{2-} assay after Na_2SO_3 treatment coupled with a positive S°_{x-1} determination is the only indicator of Sb(V) in sulphide solution that the author has found. However, the

Table 3-2: Sulphide and Polysulphide Sulphur Determinations in Antimony (V) Solution

$Na_2SbS_4 \cdot 9H_2O$ added (g/100 ml)	Sb calc. (g/l)	Sb deter. (g/l)	Sulphide Analysis		Polysulphide Sulphur Analysis		
			S^{2-} (M)	S^{2-}/Sb (mole/mole)	S^{2-}/Sb (mole/mole)	$\Delta S^{2-}/Sb$* (mole/mole)	S^{o}_{x-1}/Sb (mole/mole)
2.19	5.54	5.20	0.173	4.05	3.35	0.70	0.35
4.08	10.3	9.58	0.328	4.17	3.51	0.66	0.36
8.48	21.5	19.9	0.676	4.15	3.56	0.59	0.34
16.50	41.8	38.9	1.33	4.17	3.13	1.04	0.54

* ΔS^{2-} is the difference between the sulphide analysis and the sulphide analysis after treatment with $Na_2S_2O_3$

reduction procedure used appears only to be an indicator of Sb(V). A proper analysis would have to involve a boiling treatment with Na_2SO_3 under an inert gas cover to prevent S^{2-} oxidation.

3.3 The Determination Of Sulphur In Solids

The sulphur content of the concentrate and the leach products was determined gravimetrically by the conversion of sulphur to barium sulphate, $BaSO_4$ (Young, 1971).

3.4 Caustic Determination

3.4.1 Caustic Determination In Sulphide Solution

Caustic was determined by titration with HCl solution using a Radiometer RTS 822 titration system and a Canlab combination pH/reference electrode. The titration beaker was put under suction to take away the H_2S found during the determination.

With caustic and sulphide in solution, two end points are observed. OH^- and S^{2-} titrate simultaneously (Section 3.1) with an end point at pH 7.5 while HS^- titrates with an end point at pH 4.5. Polysulphide titrates as S^{2-} and is observed to decompose, but it is not certain whether Equation 3-9 or 3-10 describes the titration chemistry.

$$S_x^{2-} + H^+ = HS_x^- = HS^- + S^\circ_{x-1} \quad ...(3\text{-}9)$$

$$S_x^{2-} + H^+ = S^{2-} + S^\circ_{x-1} + H^+ = HS^- + S^\circ_{x-1} \quad ...(3\text{-}10)$$

Since weak bases, such as SO_3^{2-}, tend to titrate with HS^-, the titrant volume difference between the two sulphide end points (S^{2-} and HS^-) may not be meaningful. Caustic is best determined by the result of the first end point minus the S^{2-} determination.

The titrations were performed by pipetting 1 or 2 ml of sample into a titration beaker, diluting to 60 ml and titrating with 1 M HCl.

3.4.2 The Effect Of Antimony(III) On The Caustic Determination

The solutions considered in Section 3.3.2 were titrated with HCl as described in the previous section. The results are given in Table 3-3.

A 2:1 Sb(III):S^{2-} complex appeared to be present at the first end point consistent with SbS_2^- or $Sb_2S_4^{2-}$. With Sb(III) in solution, caustic is determined by the result of the first end point minus the S^{2-} determination plus twice the Sb assay.

After the first end point the solutions developed colours varying from orange to black and Sb_2S_3 precipitated after the second end point.

Table3-3: Caustic Analysis in Antimony (III) Solution

Sb_2S_3 (g/100 ml)	Sb deter. (g/l)	I ΔS^{2-}/Sb* (mole/mole)	1st. E.p. equiv. (M)	II ΔS^{2-}/Sb** (mole/mole)	I-II (mole/mole)
0			1.14 } 1.12		
0			1.10 }		
0.57	4.16	1.78	1.12	-	-
1.06	7.44	1.52	1.09	-0.43	1.95
1.53	10.8	1.43	1.08	-0.42	1.85
2.00	14.2	1.53	1.07	-0.45	1.98
2.62	18.6	1.64	1.04	-0.51	2.15
3.12	22.1	1.78	1.03	-0.50	2.22
				mean =	1.99±0.15

* taken from Table3-1

** ΔS^{2-} is the equivalent difference between the first end point titration of the blanks and the sample

3.4.3 The Effect Of Antimony(V) On The Caustic Determination

The solutions of Section 3.3 were titrated with HCl. The pH dropped instantly as the titration was begun. No free S^{2-} ions appeared to be present consistent with the Sb(V) complex, SbS_4^{-3}, in solution. The solutions immediately turned orange and and Sb_2S_5 precipitated after the 'second' end point.

3.5 Atomic Absorption And Flame Emmission Analysis

Copper, iron, antimony, zinc, arsenic and manganese were determined by atomic absorption spectrophotometry on a Perkin-Elmer 306 instrument. Sodium was determined by flame emmission on the same spectrophotometer.

For all the analyses, standards were made up to approximate the composition of the unknowns. For the concentrate and leach product analyses two sets were used: one containing copper, iron and antimony, and the other containing zinc, arsenic, sodium and manganese in a strong solution of the first three elements. This procedure greatly reduced the time required to make up standards while compensating for the flame matrix effects of the unknowns. The unknown and standard solutions were all made up in 20% HCl to prevent antimony hydrolysis.

Samples of the leach solutions and the antimony-arsenic standards were made up in 0.2 M Na_2S and 0.2 M NaOH. Care was taken to avoid mixing this Na_2S with the acids usually present

in the burner head drain reservoir.

Flexibility in sample dilution is available if the atomic absorption burner head is rotated to change the flame path length. The linear portion of each element's absorption versus concentration curve can be increased by approximately 20 times by having the burner normal to the lamp beam line rather than co-linear with it. Fewer sample dilutions are so required.

Chapter 4.

Results and Observations

4.1 Leaching Experiments Considered

Forty-seven equilibrium leaching experiments were done in total, but of these, only the results of 28 are considered in the following sections. A preliminary group of 16 contained too many inconsistencies and the results of three subsequent experiments were considered to be anomalous. Data from all 47 runs are shown in Appendix D.

4.2 Antimony Leaching - Equilibrium Results

4.2.1 Antimony Leached In Alkaline Sulphide Solutions

Figures 4-1 to 4-3 show the concentration of antimony leached after 24 hours at 100°C as a function of the final Na_2S concentration. Four levels of initial caustic concentration were investigated: 0, 0.5, 1.0, and 2.0 M . Curves were not interpolated through the data points as the final NaOH concentrations varied.

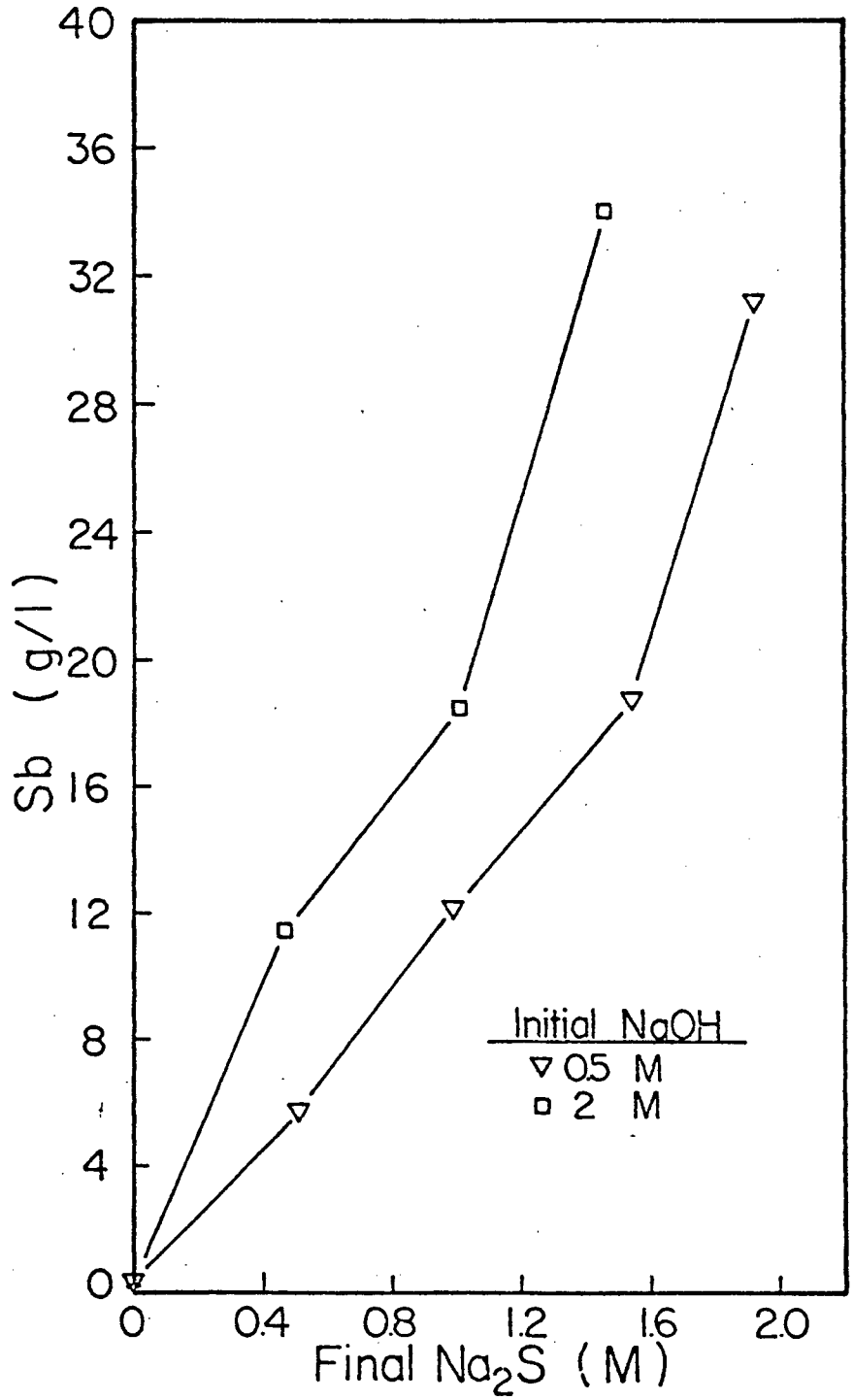

Figure 4-1 The Final Antimony Concentrations versus the Final Total Sodium Sulphide Concentrations - 0.5 and 2 M Initial Caustic

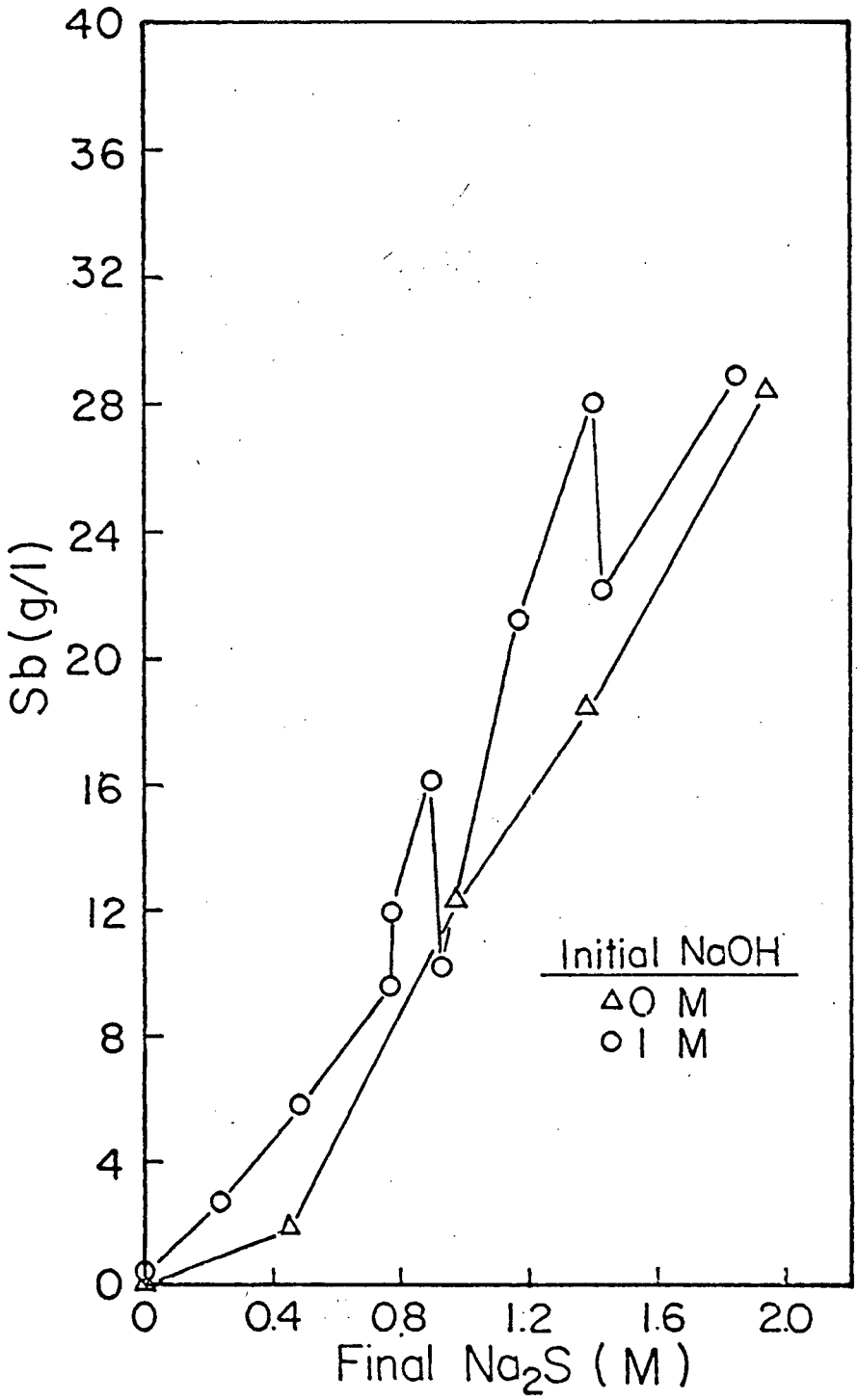

Figure 4-2 The Final Antimony Concentrations versus the Final Total Sodium Sulphide Concentrations - 0 and 1 M Initial Caustic

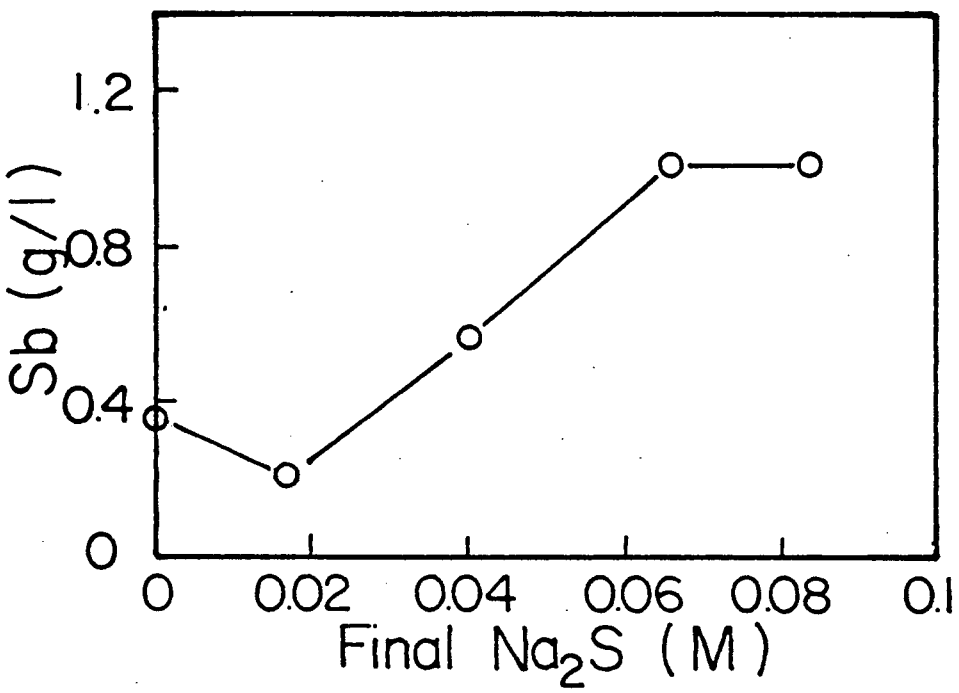

Figure 4-3 The Final Antimony Concentrations versus the Final Total Sodium Sulphide Concentrations - 1 M Initial Caustic and Low Sulphide

4.2.2 Antimony Leached In Caustic-Only Solutions

Leaching experiments were done in 0.5, 1.0 and 2.0 M NaOH solutions. Sodium sulphide was not added and no sulphide was found in any of the final solutions.

The caustic titrations of the final solutions with HCl showed two end points: one for OH^- and another which appeared to be for the neutralization of the SbO_2^- ion (Equation 4-1).

$$SbO_2^- + 4HCl = SbCl_4^- + 2H_2O \qquad ...(4\text{-}1)$$

The titrant volume difference between the two end points corresponded to a $Sb:H^+$ ratio of approximately 4 and was the same for all three solutions suggesting 0.3 g/l of Sb in solution. The total titrant volume at the second end point was approximately equivalent to the initial caustic concentration. Since the quantities of concentrate and solution charged to each of these experiments were identical, the results suggest that an antimony oxide was leached from the concentrate. However, the leaching of an oxide would increase the net caustic concentration, and this was not observed.

4.3 Leaching In Weak Sodium Sulphide Solutions Without Added Caustic

Four experiments were done at 0.03, 0.06, 0.09 and 0.12 M Na_2S without added caustic. The resultant slurries were unfilterable by the pressure and vacuum techniques described in Section 2.3. After the excess concentrate was allowed to settle the solutions were the deep green-black colour characteristic of thioferrate. Added acetone appeared to flocculate a material, presumably $NaFeS_2 \cdot xH_2O$.

Although these solutions were not quantitatively assayed, a qualitative result was obtained by SEM x-ray analysis on a drop of 0.12 M Na_2S product solution evaporated onto a carbon stub. Arsenic, silicon, antimony, iron and copper as well as sodium and sulphur were present. The iron peak was much larger than the copper peak again suggesting the presence of $NaFeS_2$.

The 0.12 M Na_2S product solution eventually flocculated as did the black filtrate from a 0.45 M Na_2S / 0 M NaOH leaching experiment. The supernatents were colourless indicating that the thioferrate present was stable. The decomposition of thioferrate would have produced a yellow supernatent solution indicative of polysulphide (Section 1.3.3). (This may be a deceptive result since polysulphide is not a stable species in alkaline solution.)

4.4 The Excess Of Concentrate Used

Excess concentrate was charged to each leaching experiment in an effort to equilibrate the solids with the solutions. Antimony extractions of less than 50% were sought. In actuality the antimony extractions varied between 8 and 62% with a mean of 35%. Only one extraction was above 50%. The extractions are tabulated with the leach data in Appendix D.

4.5 Filterability Of The Leached Product Slurry

During the leach the concentrate disintegrated into finer material which proved to be difficult to filter. These fines, together with the excess concentrate used produced a very thick product slurry, particularly in those runs which had high Na_2S concentrations. A practical experimental limit of 2 M Na_2S had to be imposed to achieve a solid/liquid separation at the end of leaching.

The pressure filtration required 25 psig of nitrogen to produce 10 ml of filtrate in 5-10 minutes. Large Buchner funnels were used to acheive reasonable vacuum filtration rates for the bulk of the solutions. During water washing of the leached solids the filtration rates dropped and what appeared to be fine solids broke through the filter paper. The SEM x-ray analyses of these solids when they eventually settled (flocculated) indicated that iron, sodium and sulphur were

present. When the leached solids were washed with a weak caustic solution instead of water, the filtration rate did not drop, nor did material break through. This filtration behavior and the SEM analyses seem indicative of the presence of sodium thioferrate.

As well as filtering poorly, the leached solids did not settle well. If allowed to sit while hot, only 5 mm of clear liquid were produced over 10 cm of slurry in 10 minutes.

4.6 The Change In Sulphide Concentration

Figure 4-4 shows the differences in the total Na_2S concentrations between the initial and final solutions plotted against the final antimony concentrations. The differences are shown on an absolute and on a relative basis. A small net drop in sulphide concentration was observed in all the equilibrium experiments except one. The absolute drop was unrelated to the antimony concentration. At low antimony (low sulphide) the relative loss rose sharply.

The one run which showed a net increase in Na_2S concentration was the only experiment in which the antimony extraction exceeded 50%. In this case the extraction was 62%.

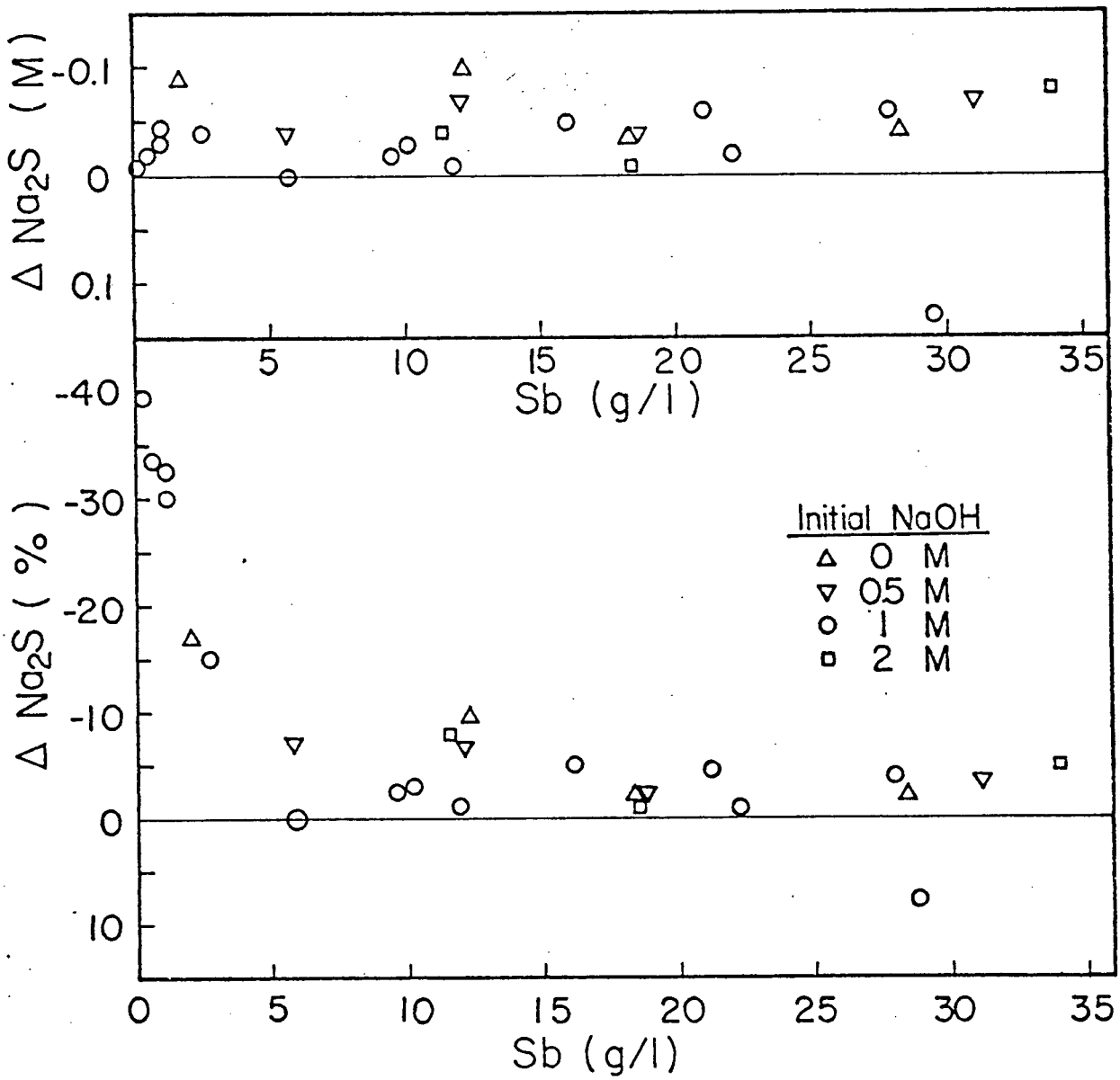

Figure 4-4 The Differences Between the Initial and Final Sodium Sulphide Concentrations-Absolute (Top) and Relative (Bottom), versus the Final Antimony Concentrations

4.7 The Change In Caustic Concentration

Figure 4-5 shows the differences in the NaOH concentrations between the final solutions and those calculated for the initial solutions as a function of the final Na_2S concentrations. An ascending solid line was fitted through the points for 0.5, 1.0 and 2.0 M initial caustic, while the broken line fitted through the points for no added caustic had a negative slope.

If the 1 M initial NaOH points of Figure 4-2 are compared against the corresponding data (Appendix D), the 'low points' appear to be associated with smaller ΔOH's than the 'high points'. Figure 4-6 shows a plot of the leach antimony concentrations plotted against the product of the final Na_2S concentrations and the final NaOH concentrations. The points of Figure 4-2 are selectively shifted producing Figure 4-6, a plot with much less scatter.

The initial NaOH concentrations were not measured but rather calculated from the added caustic. The caustic content of the Na_2S was determined to be 0.02 - 0.03 mole per mole (Section 2.1.2). A correction was not applied to the initial leach solution caustic assays.

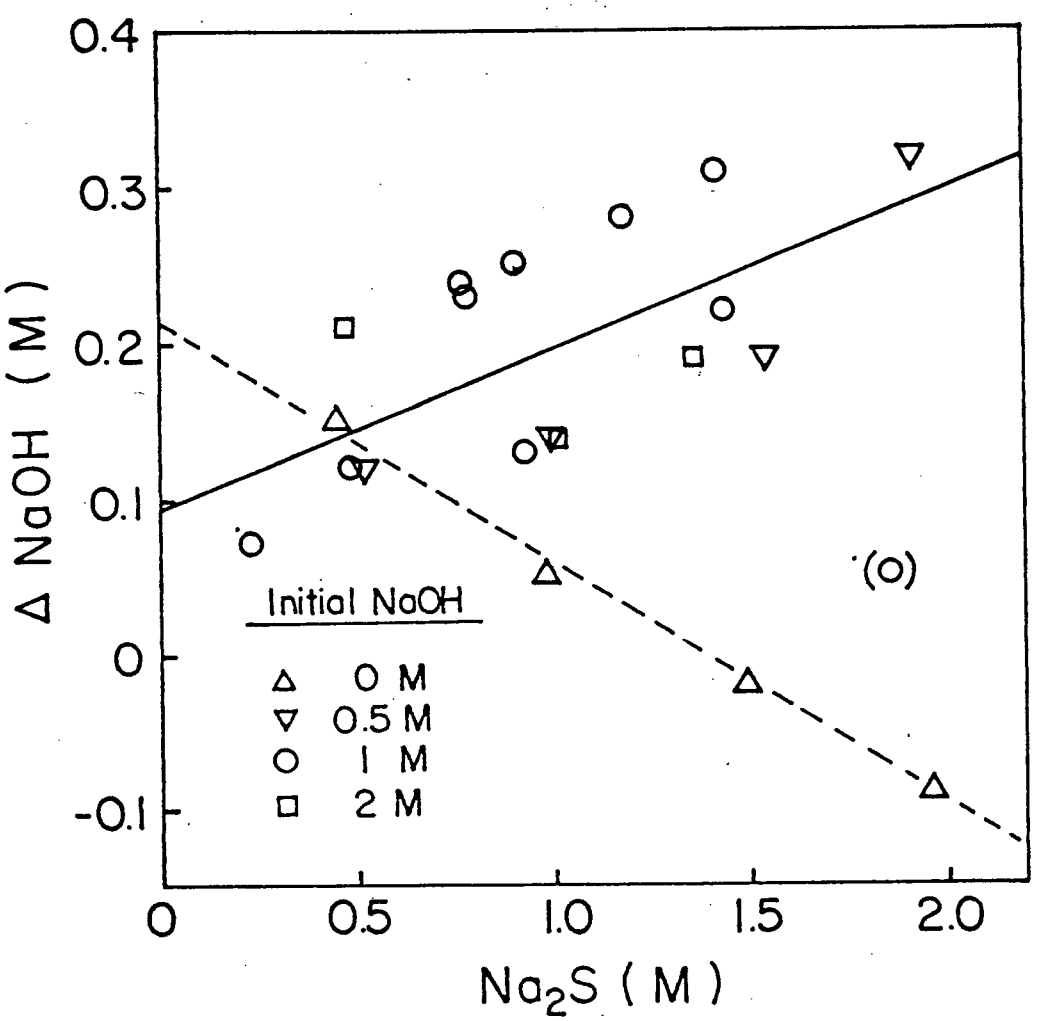

Figure 4-5 The Differences Between the Initial and Final Sodium Hydroxide Concentrations versus the Final Sodium Sulphide Concentrations

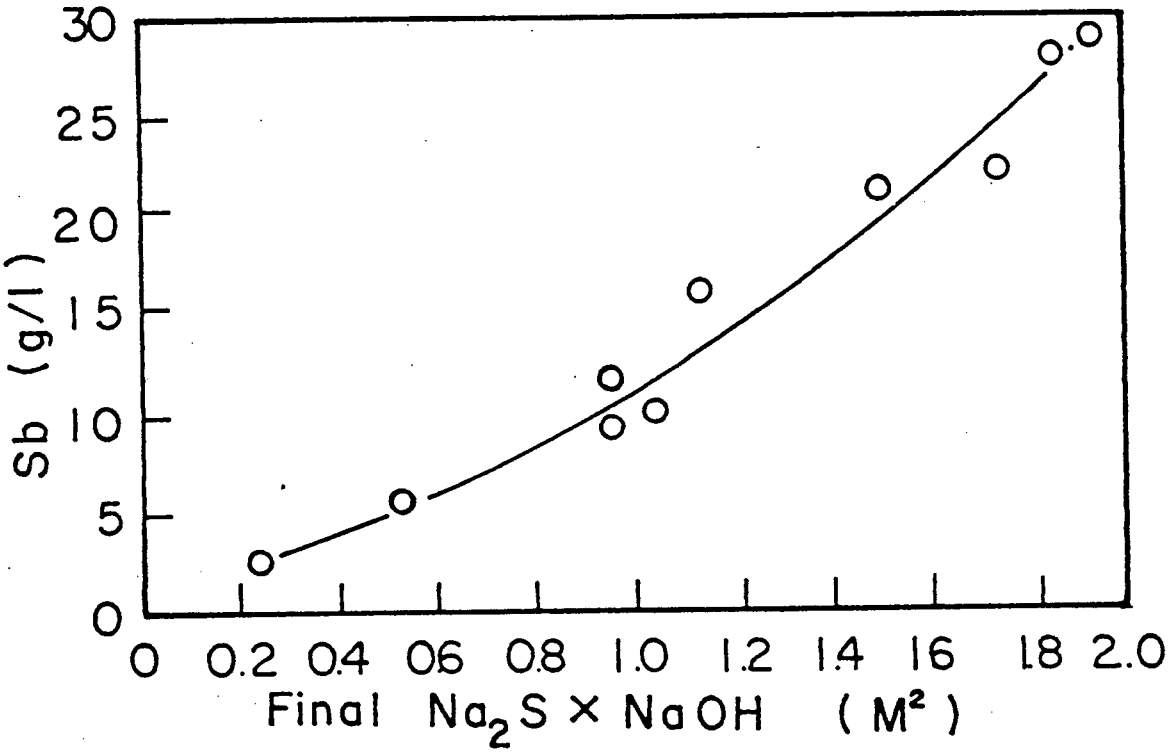

Figure 4-6 The Final Antimony Concentrations versus the Product of the Final Sodium Sulphide and Sodium Hydroxide Concentrations (1 M Initial Caustic)

4.8 Arsenic Dissolution

Figure 4-7 shows the arsenic concentrations of 12 leach solutions plotted against the antimony concentrations. Equation 4-2 was fitted through the points.

$$As(g/l) = 0.21 + 0.068\ Sb(g/l) \quad \ldots(4\text{-}2)$$

The arsenic to antimony ratio of the concentrate is represented by the broken line (Section 2.1.1). The slope of the experimental line is less than the slope of the concentrate line due to the presence of an insoluble arsenic-containing phase - most likely arsenopyrite, AsFeS. At low sulphide these lines cross because arsenic-sulphide complexes are more stable than their antimony counterparts and because there were adequate quantities of arsenic available at the exposed mineral particle surfaces. At higher sulphide levels the arsenic was only made available through the decomposition of tetrahedrite.

The zero-intercept of the fitted line (0.21 g/l As) is an artifact created by the linear least squares fit which was done. The true value is probably smaller.

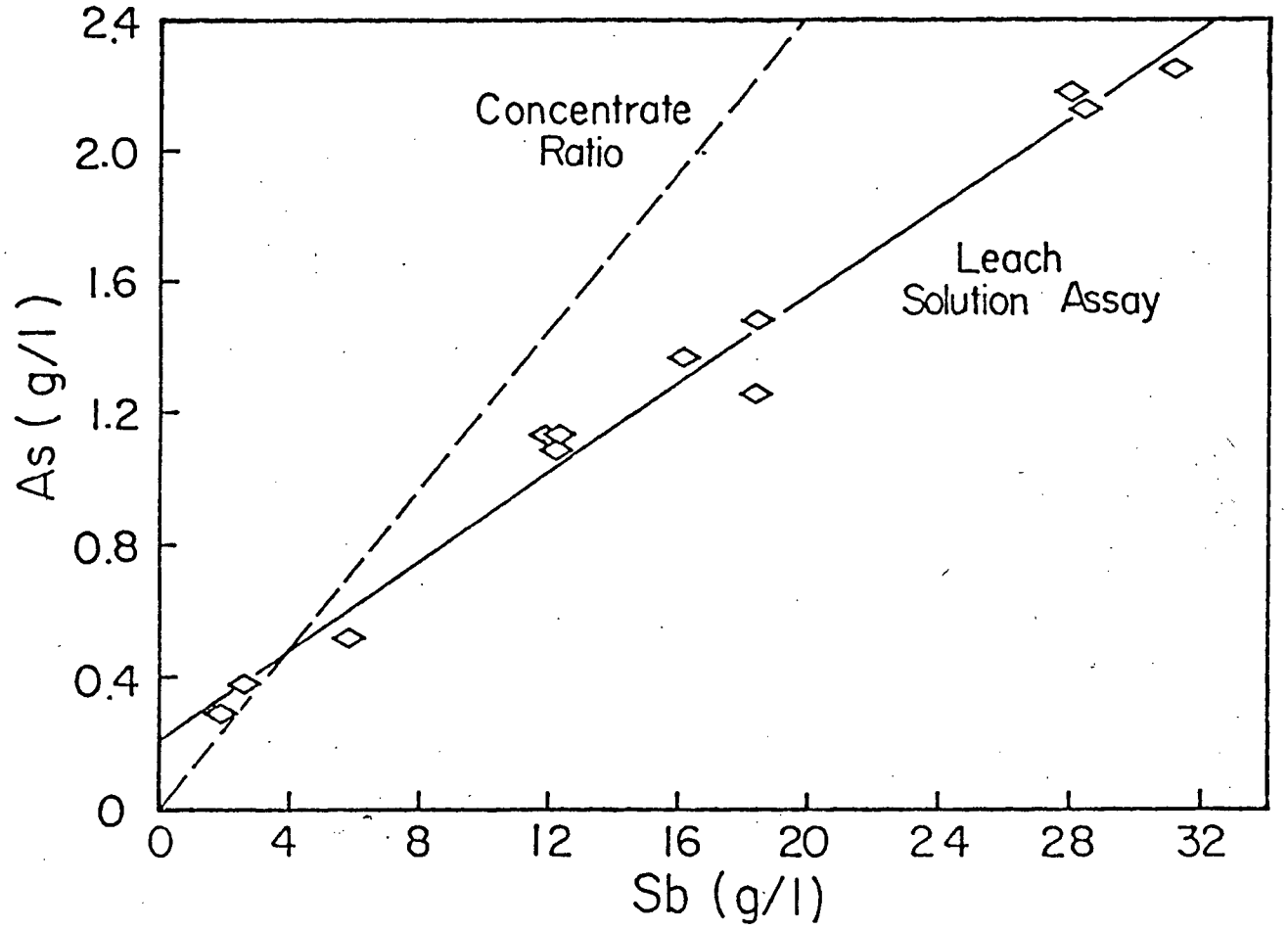

Figure 4-7 The Arsenic Versus the Antimony Concentrations

4.9 The Presence Of Oxidized Sulphur Species And Antimony(V)

The results of the analyses for oxidized sulphur species and so for Sb(V) (Section 3.2.3) did not show any systematic pattern. Considering the oxidation problems identified in the solid/liquid separation (Section 2.3) and in the S°_{x-1} determination (Section 3.2.1), it is unlikely that significant quantities of these species were present at the end of the leaches.

4.10 Antimony And Sulphide Concentrations Versus Time

Figures 4-8 and 4-9 show the antimony and sulphide concentrations of four leaching experiments plotted against time. The antimony curves show a regular rise, while the sulphide curves are more complex. The data for these runs is given in Appendix E.

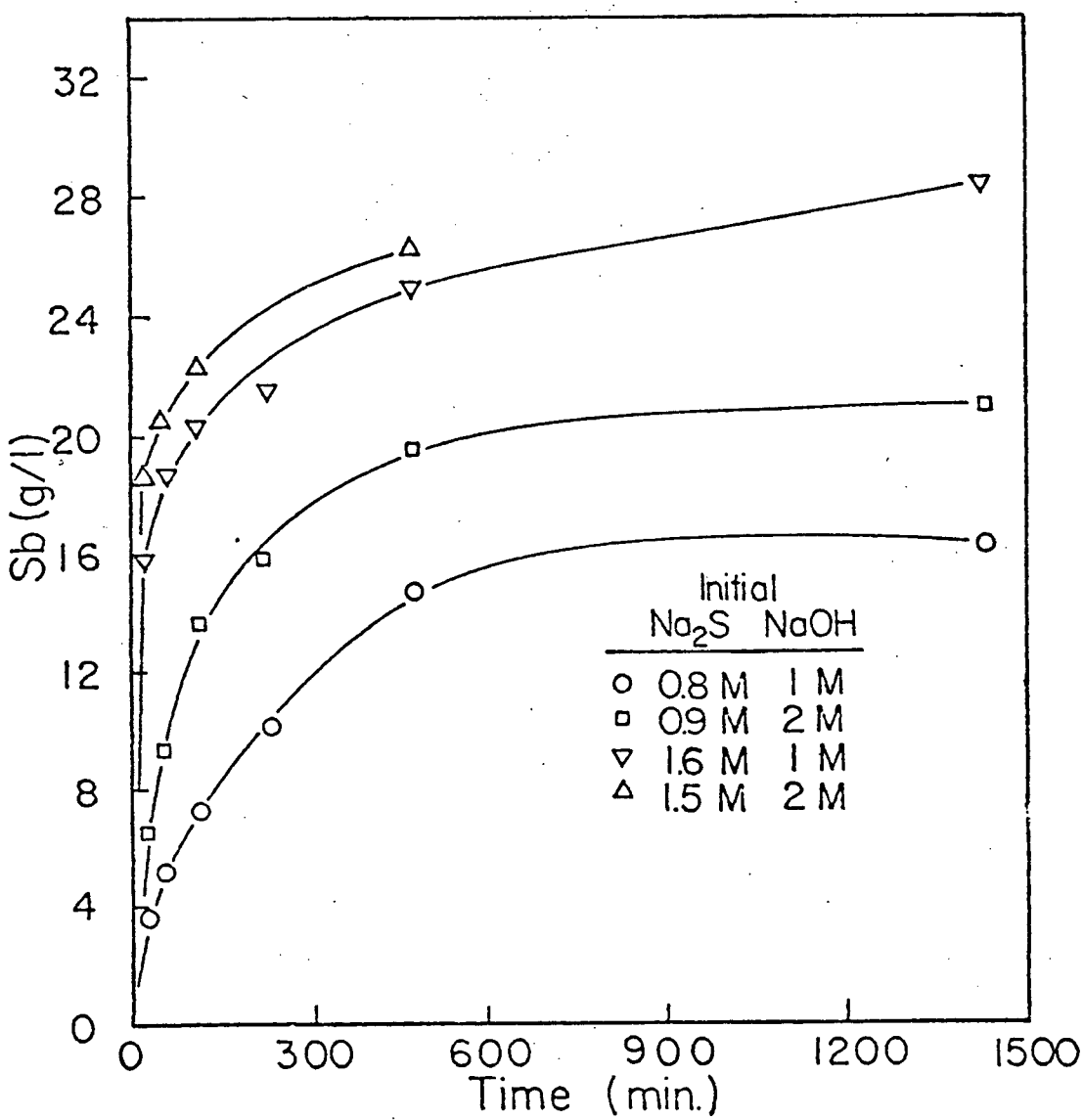

Figure 4-8 The Solution Antimony Concentrations as a Function of Time

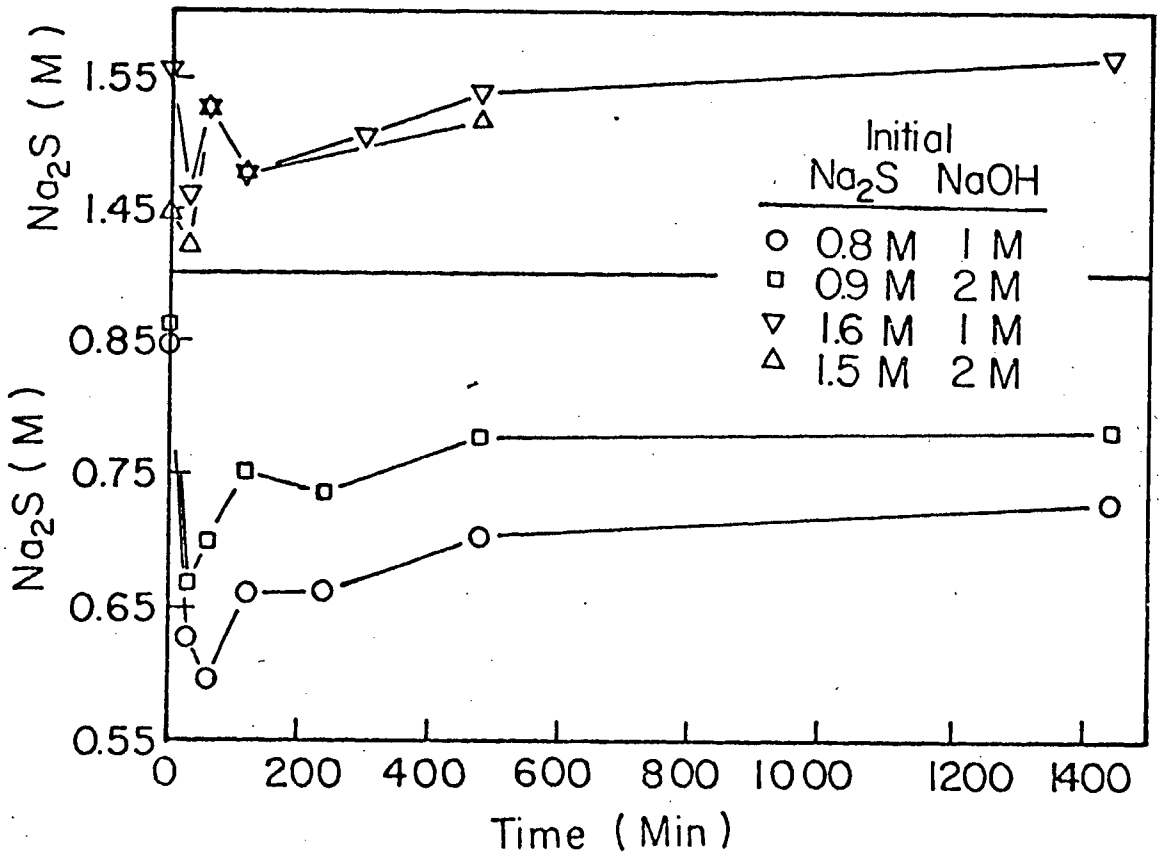

Figure 4-9 The Sodium Sulphide Concentrations as a Function of Time

4.11 Appearance Of The Concentrate And Product Solids

Figures 4-10 and 4-11 show SEM micrographs of the concentrate and the leached product solids at 2,100 and 21,000 times. (The production of the product solids is described in Table 4-2, leach 2.) The concentrate is obviously crystalline while the product solids are not. The leached particles are much less than 1 μm in size.

4.12 X-ray Diffractometry Of The Product Solids

The x-ray diffraction line pattern for the product solids was identical to the pattern for the concentrate. The concentrate decomposition product was x-ray amorphous, consistent with its 'fuzzy' appearance.

4.13 Comparison Of Tetrahedrite And The Decomposition Product By Electron Microanalysis

Figure 4-12 shows SEM x-ray analyser spectra taken from tetrahedrite and decomposition product areas on a mounted and polished sample of leached material (leach 2, Table 4-2). The spectra, containing 500,000 counts each, are shown separately and superimposed to accentuate their differences. The greatest differences are the disappearance of the antimony from tetrahedrite and the large increase of iron in the product. The

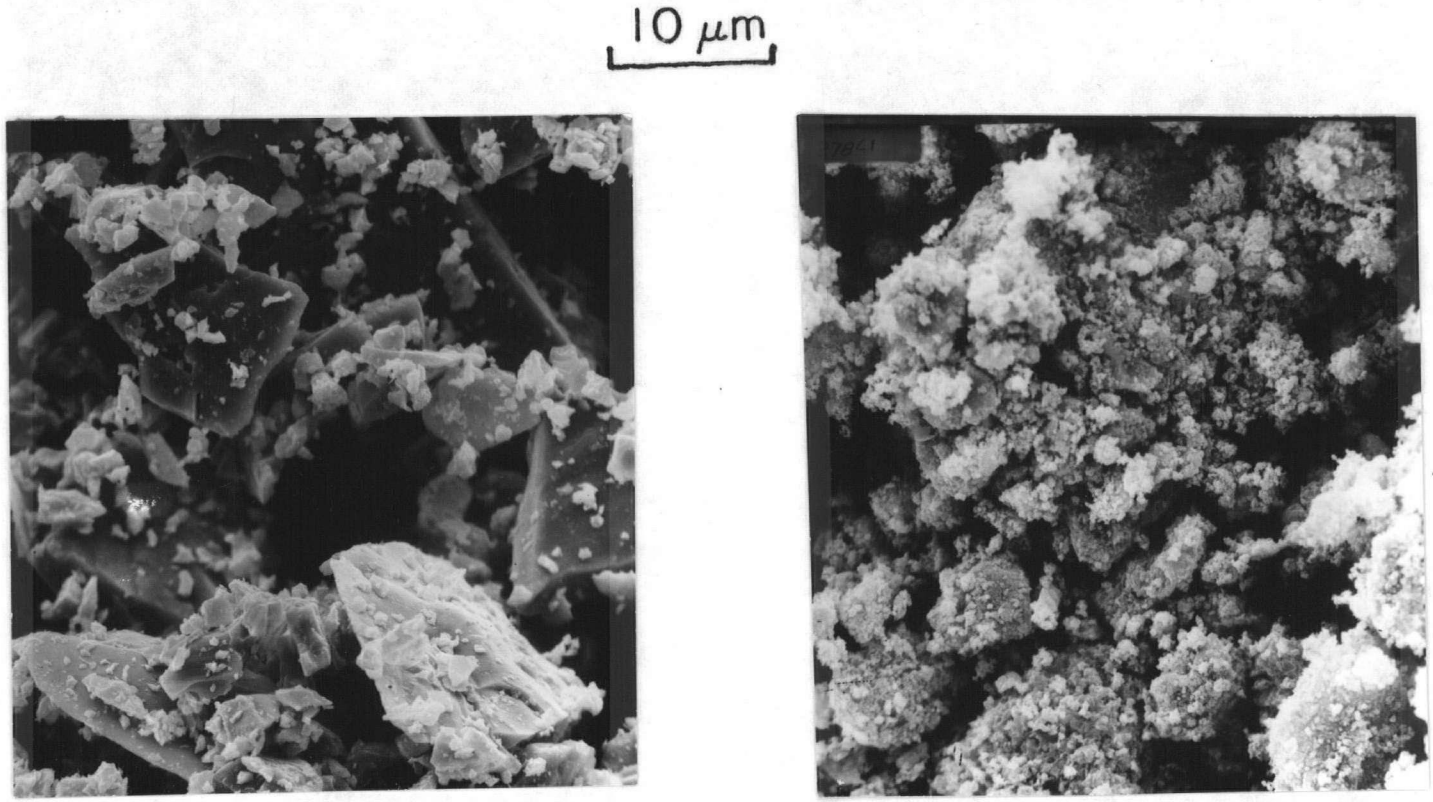

Figure 4-10 The Tetrahedrite Concentrate (a) and the Leach Product Solids (b) at 2,100 x

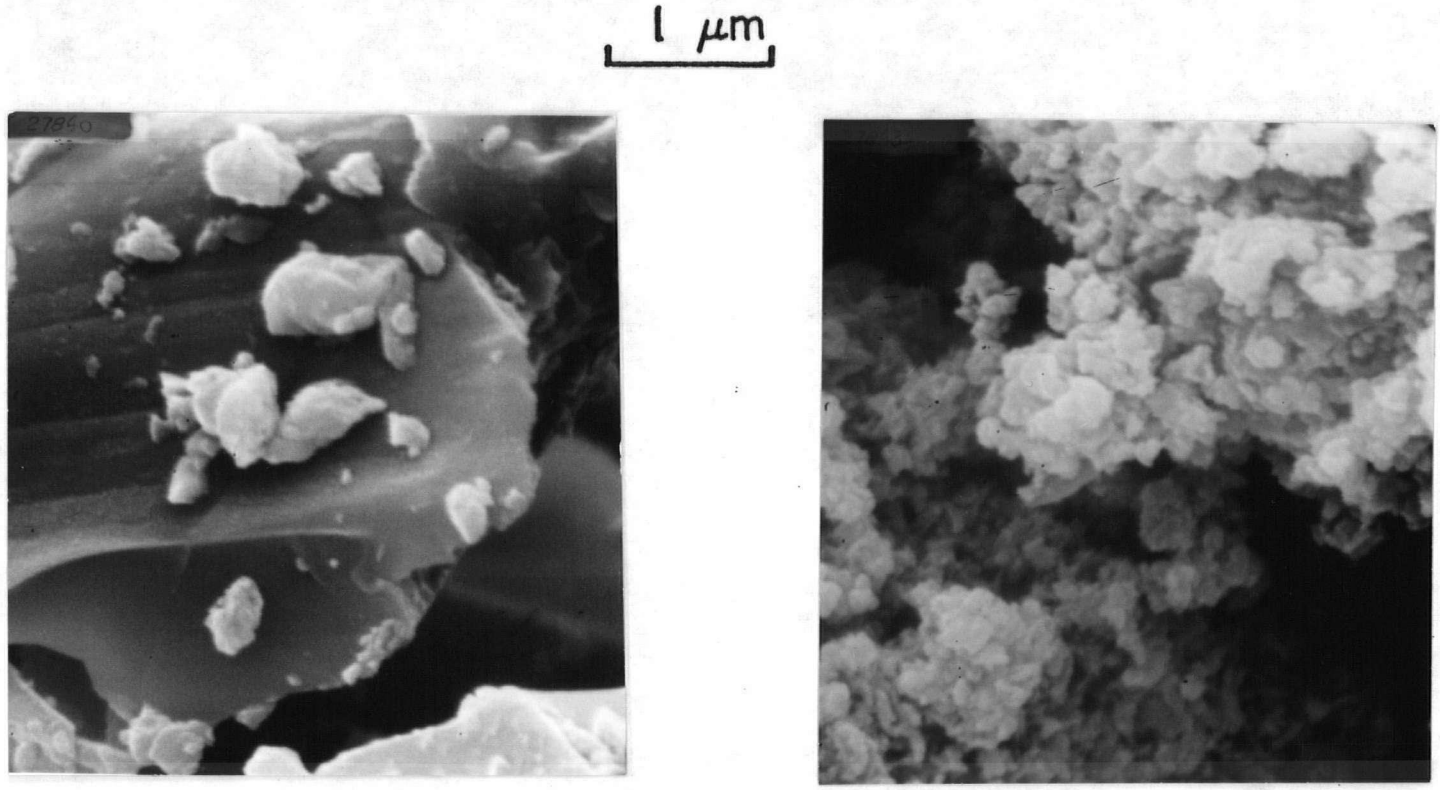

Figure 4-11 The Tetrahedrite Concentrate (a) and the Leach Product Solids (b) at 21,000 x

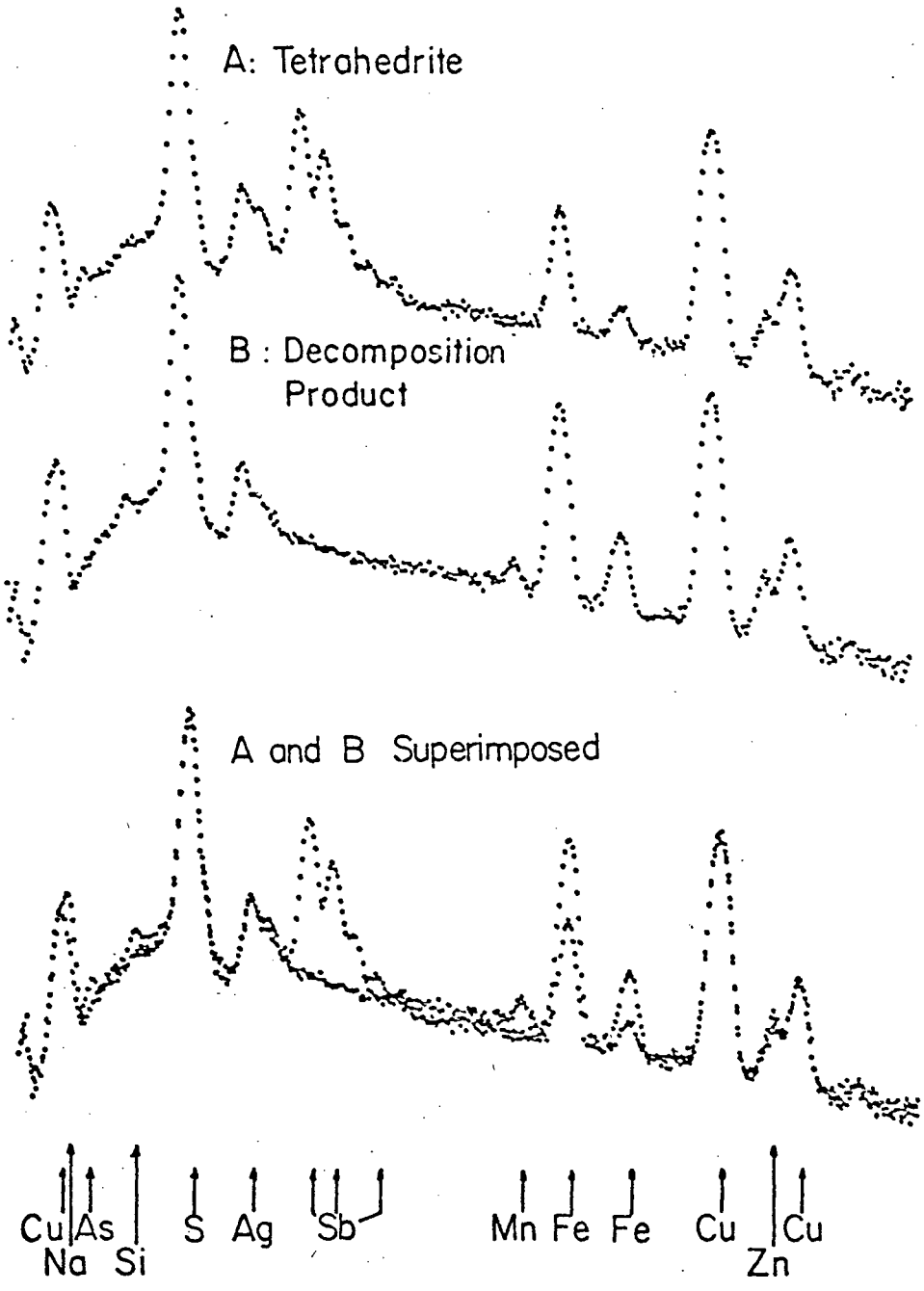

Figure 4-12 SEM X-ray Analyser Spectra for the Tetrahedrite and the Decomposition Product Phases

product also gained sodium, silicon and manganese while the tetrahedrite lost arsenic. The products show both the silver and zinc found in the tetrahedrite. (These spectra are only qualitative.)

Table 4-1 shows the results of an electron microprobe analysis on the tetrahedrite and decomposition product areas. With copper as a tie, these results indicate that within the error limits stated, one iron and one sulphur are added for each antimony extracted. The microprobe analysis computer program, Magic IV, warned that the sulphur analyses were incorrect due to a high absorption correction, more than 100%. This occurs when a light element is analysed in a heavy element matrix.

The decomposition product was fine and of varying density so it was not possible to know exactly what the beam was focused on. Despite polishing the product areas were rough since the product was soft. These factors lead to the poor precision in the decomposition product analyses. Tetrahedrite was not stable under the microprobe beam and the sample had to be moved at 50μm per minute to give a valid analysis.

Table 4-1: Microprobe Analysis Results

	Tetrahedrite (atom %)	Tetrahedrite* Cu-tie (atom %)	Decomp. Product (atom %)	(atom %)
No. of Points Analysed	8		7	
S	46.4±0.4	39.8	50±6	+10
Cu	35.0±0.5	30.0	30±6	0
Fe	5.3±0.3	4.5	20±3	+15
Sb	13.3±0.4	11.4	0±0	-11

*The tetrahedrite analyses were adjusted to use a copper tie.

4.14 Leaches At Low Pulp Density

Table 4-2 shows the leaching conditions and results from three low pulp density leaching experiments. Leaches 1 and 2 were duplicates done at 100°C. Leach 3 was done at 200°C under 200 psig of nitrogen in a small shaking autoclave. In these experiments the tetrahedrite should have decomposed completely before equilibrium with the solution was attained.

Leaches 1 and 2 produced significantly different antimony dissolution results, 2.27 versus 2.73 g/l Sb. The antimony concentrations were well below those observed in the corresponding excess concentrate experiment, 12 g/l Sb. However, the equilibrium experiment was done with 50 g of wet concentrate for 130 ml of leach solution against 5 g in 125 ml in the low pulp density runs. The antimony extractions of leaches 1 and 2 were only 42 and 46%, figures which are unrealistically low in view of their apparent departure from equilibrium.

All the leach product solids contained quantities of sodium too high to be justified on the basis of entrained leach solution. These solids appeared to have contained 25 - 60 wt. % leach solution while wet though they all had been thoroughly filtered and washed. The 200°C product was easiest to filter but contained the most sodium.

The Cu:Fe and S:Fe ratios of the leached solids both dropped compared to the concentrate - slightly for the 100°C and

Table 4-2: Data and Results from Low Pulp Density Leaching Experiments

Leach	1	2	3	Concentrate
Temp (C)	100	100	200	
Time (hr)	24	24	4	
Conc (g-wet)	5.00	5.00	5.00	
Conc (g-dry)	4.63	4.63	4.63	
Leach vol (ml)	125	125	50	
Na_2S (M)	0.964	0.967	0.972	
Product (g-dry)	4.38	4.40	(3.84)*	
Sb(%)	6.7	6.1	3.9	13.1
Cu(%)	26.7	26.7	28.8	26.0
Fe (%)	15.4	15.6	17.6	14.6
S (%)	30.1	30.2	32.2	29.1
Na(%)	1.09	1.33	2.84	0.0
Solution Sb(g/l)	2.27	2.73	9.32	
Final Na_2S (M)	1.031	0.996	0.975	
Sb (out)/Sb (in)	0.95	1.01	1.02	
Sb (solids)/Sb (in)	0.48	0.44	0.25	
Na (solids)/Sb(sol'n) (mole/mole)	0.89	0.91	1.24	
Leach Soln equiv to Na (ml)	1.1	1.3	2.5	
Solids Cu/Fe (g/g)	1.73	1.71	1.64	1.78
Solids S/Fe (g/g)	1.94	1.96	1.83	1.99

*weight calculated from Fe balance; portion of sample lost.

significantly for the 200°C leach. The copper may have leached while the sulphur may have oxidized to sulphate.

4.15 Inconsistency Of Sodium In The Concentrate Decomposition Product

Sodium microanalyses were attempted, but the sodium was not uniformly dispersed and was observed only in some of the decomposition product areas. Also the apparent number of the sodium areas changed each time the sample was repolished. (The polishing was done down to 5 μm grit without the use of water.) These observations were made by taking SEM x-ray analyser spectra such as Figure 4-11. When a microprobe analysis was attempted no area could be found where the sodium x-ray count was more than twice the background. Twice the background is considered to be the minimum for a valid analysis.

The decomposition product was so fine and soft that these areas were difficult to polish flat. Sodium x-rays are relatively weak and readily absorbed by heavier elements, so a flat sample surface is essential to their detection.

4.16 The Sodium To Antimony Ratio Of The Leached Solids Wash Water

To investigate the disposition of sodium during the washing of the leached solids, a leach slurry was filtered on a Buchner funnel and water washes of 100 ml were sucked through the cake. As a control a slurry of cellulose filtering pulp was made up with the leach filtrate and then filtered and washed in a similar manner. Each solution was assayed for Na and Sb.

Table 4-3 shows the results of the washing experiments. The Na:Sb ratio of the leach solid wash solutions clearly increased relative to the controls. Sodium must have been liberated from a solid phase in the leached material to account for this result. Experiments were attempted in which the filtered solids were repulped after each wash. The solids proved to be difficult to disperse and the resultant slurries were virtually impossible to filter. Solids broke through even two fine filter papers. Solid breakthroughs were observed in the displacement washes reported above and in the equilibrium leaching experiments (Section 4.5).

Table 4-3 : Results from Filter Cake Washing

	Sb(ppm)	Na(ppm)	Na/Sb
Leached Solids:			
Leach Solution	14500	293000	20.2
Wash 1	760	16000	21.1
Wash 2	2.8	546	195
Wash 3	1.0	280	280
Cellulose Filter Pulp (control):			
Leach Solution	10400	200000	19.2
Wash 1	1390	25700	18.5
Wash 2	22.5	590	26.2
Wash 3	0.8	20	25.0

4.17 Pyrite Leaching

A sample of coarse crushed pyrite was leached in 0.03 M Na S for six hours at 100°C. The resultant solution was a deep green-black colour suggestive of sodium thoiferrate. A similar sample of pyrite was treated with cold 1% HCl to remove oxides, and rinsed thoroughly with water. A 1 M Na S solution was added and immediately turned black. After 12 hours of leaching at 100°C the solution had darkened significantly. Acetone added to a hot solution sample flocculated the thioferrate and no polysulphide yellow was observed. A SEM x-ray analysis on a drop of flocculated solution indicated the presence of sodium, sulphur, silicon and iron. The bulk of the solution flocculated thioferrate upon cooling but appeared to redisperse when heated to boiling.

4.18 Silica-Iron Oxide Particles

Figure 4-13 shows a SEM micrograph of a silica-iron oxide particle in the concentrate and its Si and Fe x-ray energy maps. The bright areas on each map indicate the sources of the x-rays for the element under consideration. The x-ray spectrum, from a dark grey area showed silicon with much smaller iron and copper peaks while the light grey area showed iron, copper and manganese (but no sulphur). This phase is the only source of manganese in the concentrate and is presumably the source of manganese in the decomposition product. Particles such as these

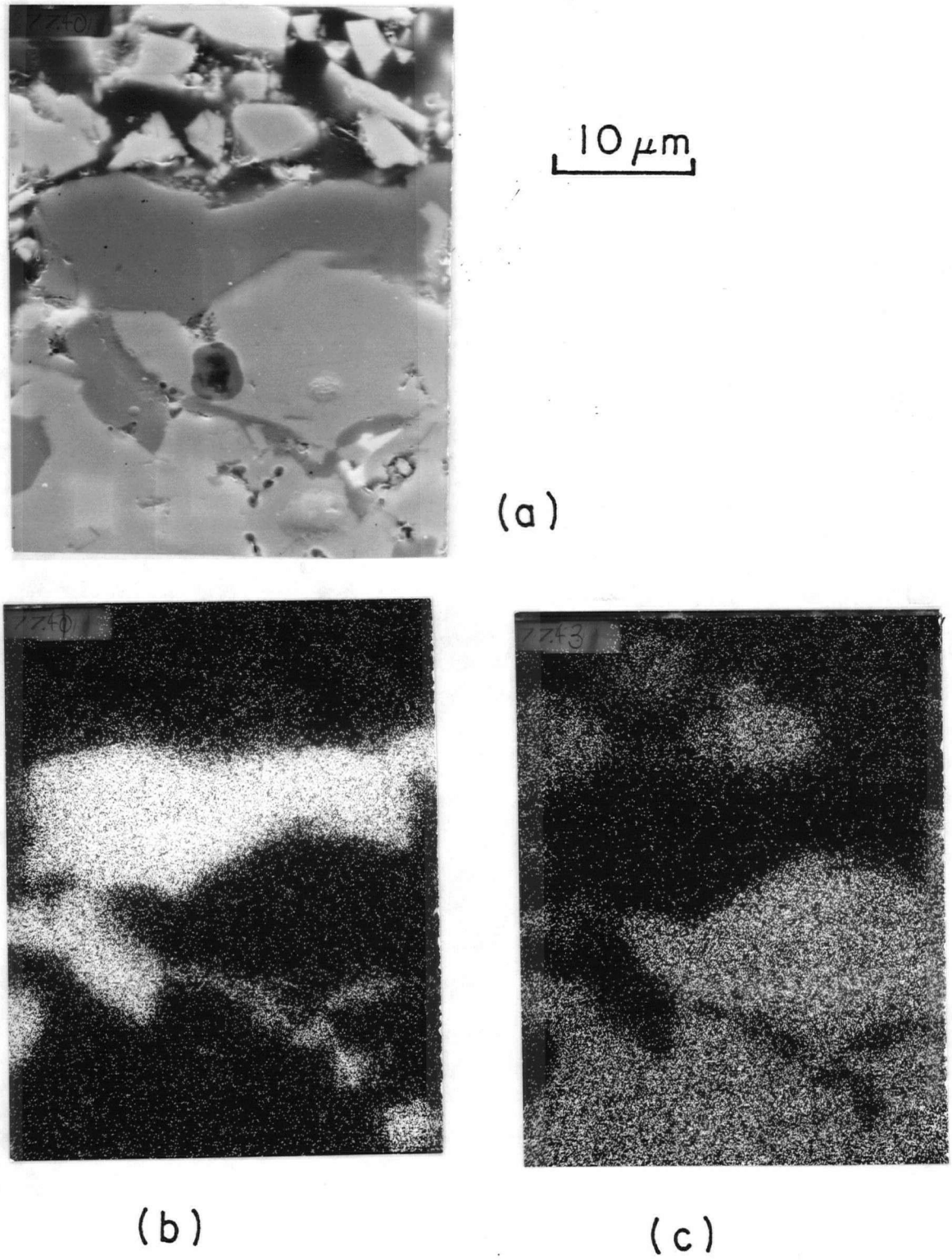

Figure 4-13 SEM Micrograph of a Silica-Iron Oxide Particle (a) and the Corresponding Silicon (b) and Iron (c) X-ray Energy Maps

were not found in the leached material.

Chapter 5.

Dependency of Antimony Solubility on Sulphide Ion Concentration

5.1 Stibnite Solubility Plots

Although there is a lack of agreement as to which antimony(III)-sulphide complex(es) is formed from Sb_2S_3 dissolution in sulphide solutions, the literature gives experimental results which merit further analysis. No original Sb_2S_3 dissolution data was produced in this study.

If SbS_2^- is considered to be the stable Sb(III) complex in solution, then a plot of the log of the activity of the SbS_2^- ion versus the log of the activity of the sulphide ion (log $a(SbS_2^-)$ versus log $a(S^{2-})$ should be a straight line with a slope of 0.5 (Equations 5-1 to 5-3). However, concentrations rather than activities are experimentally determined and activity coefficient data has not been published for HS^-, S^{2-} or any Sb(III)-sulphide complex.

$$1/2\ Sb_2S_3 + 1/2\ S^{2-} = SbS_2^- \qquad ...(5\text{-}1)$$

$$K(SbS_2^-) = \frac{a(SbS_2^{2-})}{a^{0.5}(S^{2-})} \qquad ...(5\text{-}2)$$

$$\log a(SbS_2^-) = 1/2 \log a(S^{2-}) + \log K(SbS_2^-) \quad ...(5\text{-}3)$$

On a concentration basis Equation 5-4 is analogous to Equation 5-3.

$$\log\{SbS_2^-\} = 1/2 \log\{S^{2-}\} + \log \gamma \frac{^{0.5}(S^{2-})}{\gamma(SbS_2^-)} + \log K(SbS_2^-) \quad ...(5\text{-}4)$$

Since each activity coefficient, γ, is a function of the total ionic strength (among other factors) it is a common experimental device to add a large concentration of inert ions to keep the reagent activity coefficients virtually constant.

The stibnite solubility data given by Arntson et al. (1966) was converted into a concentration-based log plot format for the species: SbS_3^{2-}, $Sb_2S_4^{2-}$, $Sb_2S_5^{4-}$ and $Sb_4S_7^{2-}$. SbS_2^- has the same antimony to sulphide ratio as $Sb_2S_4^{2-}$. No one has proven that both ions exist and $Sb_2S_4^{2-}$ seems more likely by a bonding argument (Section 1.3.2). A summary of the calculation scheme and the results are shown in Appendix F. The free S^{2-} ion concentration was obtained by subtracting the appropriate number of moles of sulphide per mole of antimony for the complex considered and then calculating the HS^--S^{2-}-OH^- equilibrium at 25°C. This calculation parallels the one that was used for Figure 1-3, Section 1.3.1

The results indicate that SbS_3^{3-} cannot exist in high free S^{2-} solution - the total S^{2-}:Sb ratio fell below three. In an electrochemical study Shestiko and Demina (1971) suggested that SbS_3^{3-} was stable in the region shown in the lower right hand corner of Figure 5-1. The dashed line only connects their

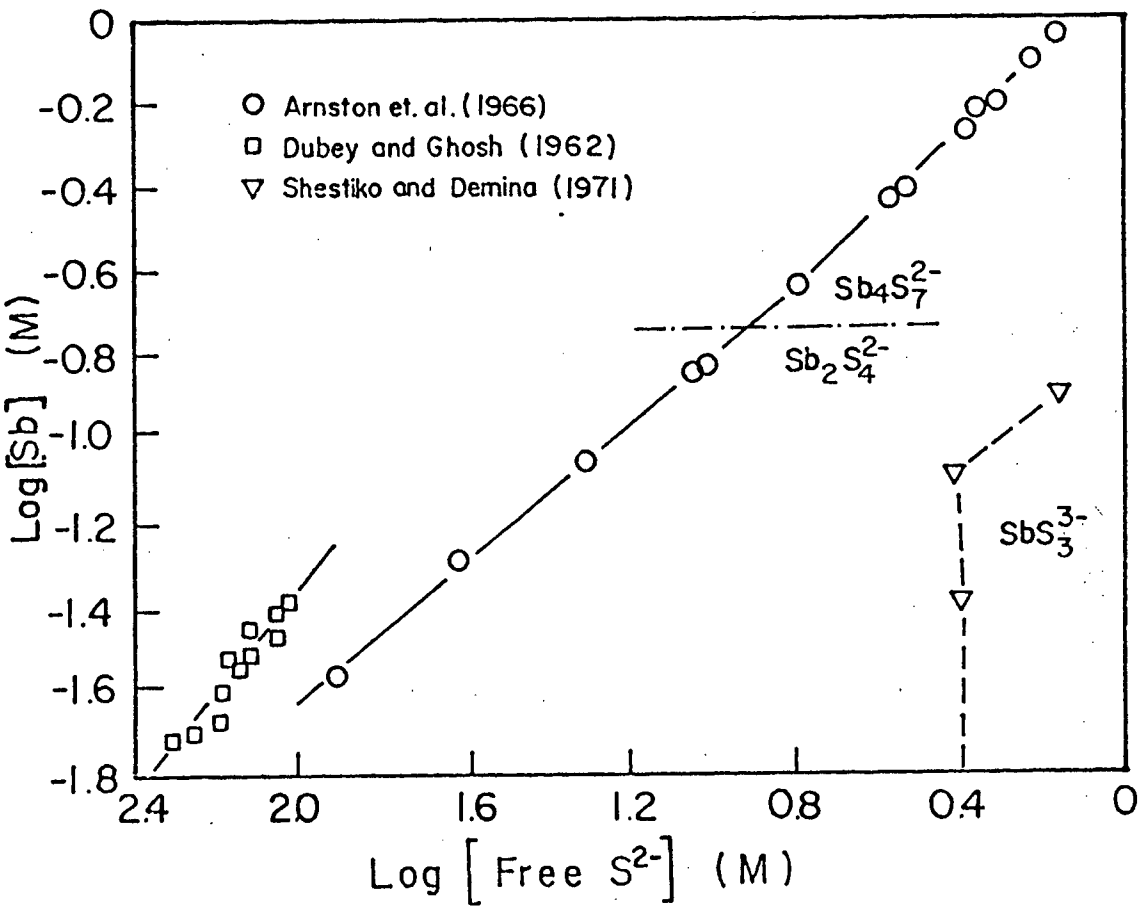

Figure 5-1: The Literature Stibnite Leaching Data Plotted Considering $Sb_2S_4^{2-}$ at Low Sulphide and $Sb_2S_7^{2-}$ at High Sulphide (SbS_3^{3-} Stablility Area Shown)

experimentally derived points and does not mean to infer a relationship between SbS_3^{3-} and other complexes. $Sb_2S_5^{4-}$ and $Sb_4S_7^{2-}$ were indicated to be stable to the left of this region. This work indicates that SbS_3^{3-} could not have been present in the solutions studied by Arntson et al. (1966).

Shestiko and Denina(1971) studied the rest potential of a metallic antimony electrode in solutions containing various concentrations of sulphide and dissolved antimony. The slopes of the lines on a potential versus total sulphide plot showed 'knees' at the ulphide level where the dominant Sb(III)-sulphide complex(es) changed from $Sb_2S_5^{4-}$ and $Sb_4S_7^{2-}$ to SbS_3^{3-}. These 'knee' points are shown on Figure 5-1.

The results of the free S^{2-} calculation for $Sb_2S_5^{4-}$ became erratic at high S^{2-} though the S^{2-}:Sb ratio did not fall below 2.5. The existence of this complex is also considered to be dubious in the solutions studied by Arnson et al. (1966).

The solubility log plots for the complexes $Sb_2S_5^{2-}$ and $Sb_2S_7^{2-}$(Appendix F) both show discontinuities at log {Sb} = -0.7. However, this discontinuity disappears if the data for $Sb_2S_4^{2-}$ at low sulphide is plotted with the data for $Sb_4S_7^{2-}$ at high sulphide (Figure 5-1). The predominant Sb(III)-sulphide complex appears to change from $Sb_2S_4^{2-}$ to $Sb_2S_7^{2-}$; a logical transition, as the more complex ion forms in stronger solutions. A 1:2 Sb(III) to sulphide complex at low free S^{2-} was suggested in the caustic titrations studies (Section 3.4.2).

For both species the idealized slopes of the corresponding

log plots should be one (Equations 5-5 to 5-9).

$$Sb_2S_3 + S^{2-} = Sb_2S_4^{2-} \quad ...(5\text{-}5)$$

$$\{Sb\} = \{Sb_2S_3^{2-}\} \times 2 \quad ...(5\text{-}6)$$

$$\log(\{Sb_2S_4\}\times 2) = \log\{S^{2-}\} + \log K(Sb_4S_7^{2-}) + \log 2 + \log \frac{\gamma (S^{2-})}{\gamma (Sb_2S_4^{2-})} \quad ...(5\text{-}7)$$

$$2\ Sb_2S_3 + S^{2-} = Sb_4S_7^{2-} \quad ...(5\text{-}8)$$

$$\log(\{Sb_4S_7^{2-}\} \times 4) = \log\{S^{2-}\} + \log K(Sb_4S_7^{2-}) + \log 4 + \log \frac{\gamma (S^{2-})}{\gamma (Sb_4S_7^{2-})} \quad ...(5\text{-}9)$$

The $Sb_2S_4^{2-}$ region has a slope of 0.81; the $Sb_4S_7^{2-}$; 0.97. The differences between these slopes and unity can be attributed to activity effects. Even the weakest solution in this series had a total ionic strength of 0.12 molal - a strength high enough to require corrections beyond the Debye Huckel term first range.

On a concentration basis $K(Sb_2S_4^{2-})$ was calculated to be 0.95 ± 0.15 (95% confidence level) in the low sulphide range and $K(Sb_4S_7^{2-})$ was 0.34 ± 0.01. The K values may also be affected by activity coefficient changes.

Arntson *et al.* (1966) believed that $Sb_4S_7^{2-}$ existed in solution. However, the $K(Sb_4S_7^{2-})$ value given in their paper is not comparable to the result above as their value was calculated for Equation 5-10 assuming the total hydrolysis of S^{2-}.

$$2\ Sb_2S_3 + HS^- + OH^- = Sb_4S_7^{2-} + H_2O \quad ...(5\text{-}10)$$

Their quoted $K(Sb_4S_7^{2-})$ value of 5 translated to 0.42 using the thermodynamics of Appendix F applied to Equation 5-8.

The results of Dubey and Ghosh (1962) are also shown on Figure 5-1 after calculations given in Appendix F. Their work, done at 30°C (and calculated as if at 25°C), was interpreted in terms of the $Sb_2S_4^{2-}$ ion - the species they believed to be in solution. The slope of the line from their results was 1.22 with a $K(Sb_2S_4^{2-})$ value of 2.01 ± 0.13. Their reported $K(Sb_2S_4^{2-})$ value was 120 based on an erroneous sulphide hydrolysis constant. The same data in terms of the currently accepted hydrolysis constant yields a $K(Sb_2S_4^{2-})$ value of 1.2. KCl was added to fix the activity coefficients of the species in their study, and was undoubtedly responsible for the poor match between their results and those of Arntson et al. (1966). Dubey and Ghosh (1962) used two levels of added KCl: 0.5 and 1.0, however, the lack of difference between these two sets seems anomalous in view of the difference between the two studies.

5.2 Tetrahedrite Solubility Plots

A treatment analogous to the one used for the published stibnite data in the preceeding section was used to analyse the tetrahedrite results generated in this work. The Sb(III)-sulphide complexes present in solution were not expected to be the same as those found in the stibnite results since the S^{2-}:Sb ratios are much higher (Sb_2S_3 at 25°C is more soluble than tetrahedrite at 100°C).

The results of the tetrahedrite equilibrium studies were converted into a solubility log plot format with log {Sb} versus log{total Na_2S}, log{free S^{2-}} and log{residual free S^{2-}} considering the complexes: $Sb_4S_7^{2-}$, $Sb_2S_4^{2-}$, $Sb_2S_5^{2-}$ and SbS_3^{3-}. In all cases a correction for arsenic in solution was made assuming AsS_2^- was present (Section 4.8). The HS^- - S^{2-} - OH^- equilibrium at 100°C was calculated to determine the free S^{2-} concentration after the appropriate number of moles of S^{2-} per mole of Sb were deducted for the complex under consideration. The calculations and their results are shown in Appendix G.

Analysis of the log plots produced was not very useful. No complexes were excluded by virtue of the S^{2-}:Sb ratios of the solutions and the scatter of the points on each plot was comparable.

For 1 M initial caustic there is a full range of log-log data (Figure 5-2) and a discontinuity appears to be present at log{Sb} = -1.05 or log{Sb} = -1.35 depending on the

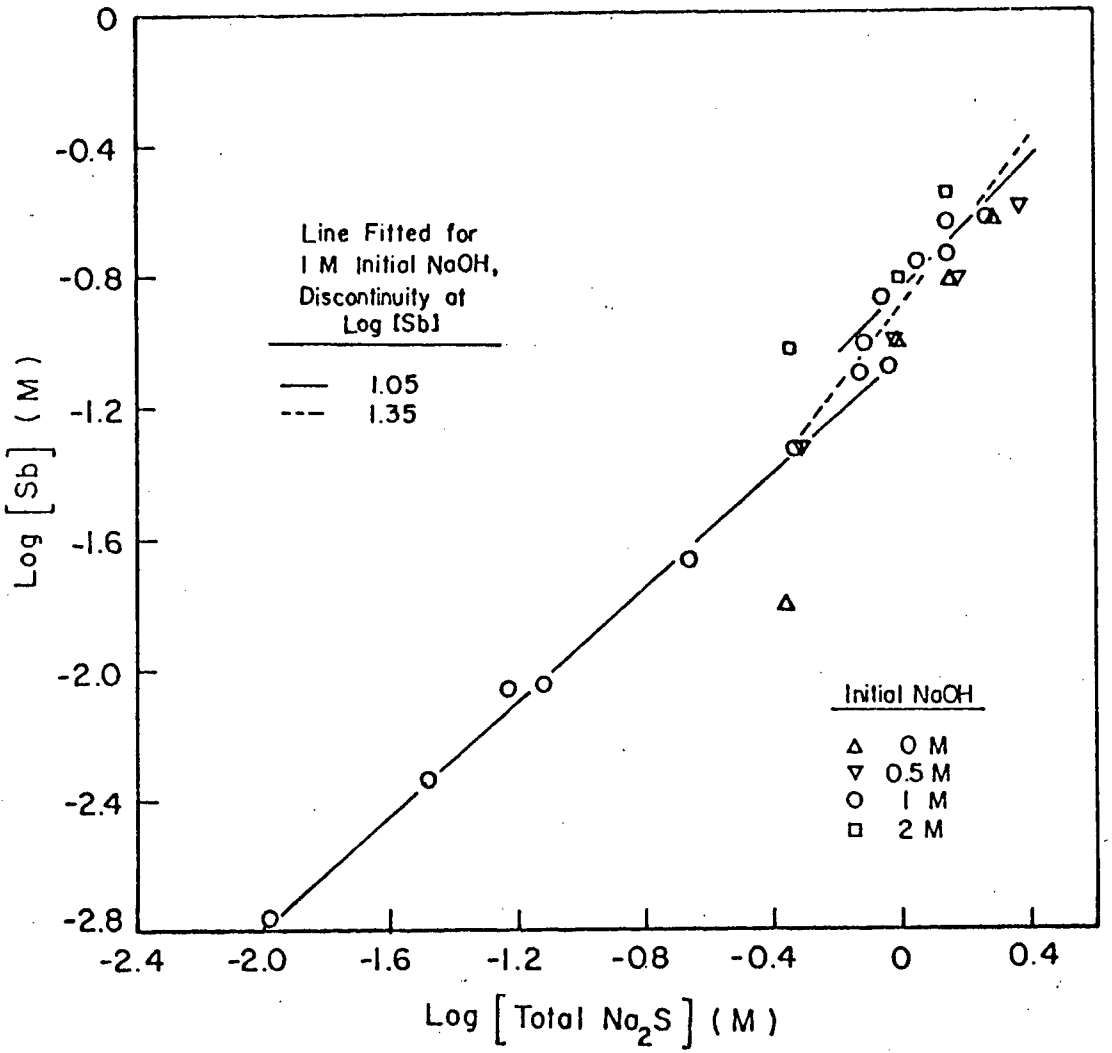

Figure 5-2 Solubility Plot for Tetrahedrite Experimental Results

interpretation chosen. In the first case the discontinuity appears as a gap between parallel lines, but a gap so wide that assigning different complexes to the sides cannot close it. In the second case, the data forms two intersecting lines, but lines that intersect regardless of the choice of complexes making up the pair. Figure 5-3 is a plot with $Sb_2S_4^{2-}$ assumed at low S^{2-}; $Sb_4S_7^{2-}$ at high S^{2-}.

Figures 5-2 and 5-4 show log{Sb} versus log {total Na_2S} corrected for AsS_2^-. These plots are intended to show the results rather than to express an equilibrium relationship. Table 5-1 gives the slopes and mean Sb/Na_2S values for various portions of the two figures. The slopes above log{Sb} = -1.05 decrease with increasing initial caustic and the mean Sb/Na_2S values increase. These effects may be real, due to the scatter of the data or due to activity effects. All the slopes measured approximated unity.

Figure 5-5 is a plot of Sb/Na_2S versus log{Sb}. At low antimony concentrations the arsenic corrections were relatively large and the unadjusted values are also shown. At high antimony concentrations the data are sufficiently scattered so that the points for different initial caustics are intermixed. The 1 M initial caustic points show an upward 'jump' at log{Sb} = -1.0. (The discontinuity in Figure 5-2 gives the same information.) A change such as this would occur if a change in the dominant Sb(III)-sulphide complex occured at this concentration.

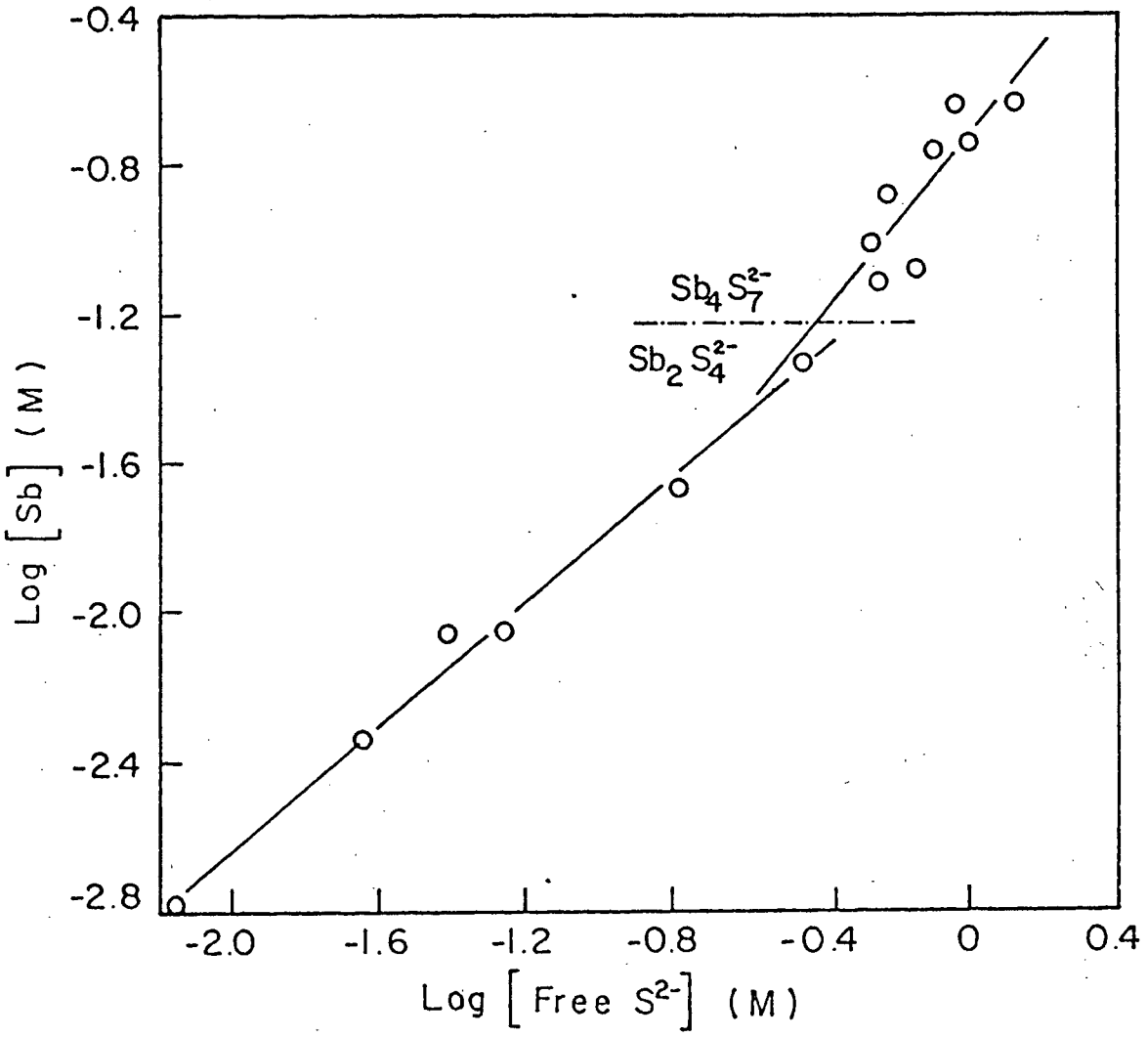

Figure 5-3 Experimental Results Plotted for the $Sb_2S_4^{2-}$ Ion at Low Sulphide; $Sb_4S_7^{2-}$ Ion at High Sulphide

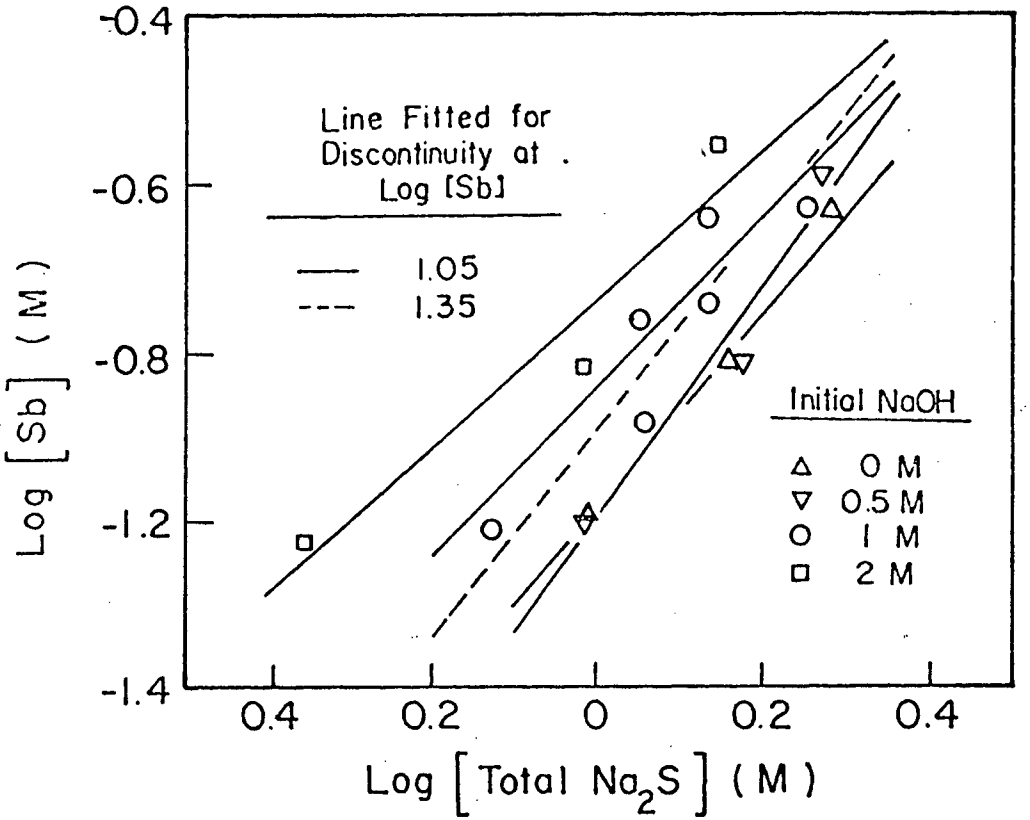

Figure 5-4 Solubility Plot for Tetrahedrite Experimental Results (High Sulphide)

Table 5-1: Mean Antomony to Sulphide Ratios and Slopes taken from Figures 5-2 and 5-4

Initial NaOH (M)	log{Sb} (log M)	Mean Sb/Na_2S* (As Corrected) (mole/mole)	Slope
0	>-1.05	0.111	1.19
0.5	>-1.05	0.115	1.37
1.0	>-1.05	0.120 0.019	1.00
2.0	>-1.05	0.190	0.89
1.0	<-1.05	0.145 0.014	0.89
1.0	>-1.3	0.134 0.020	1.26

* 95% confidence limits given

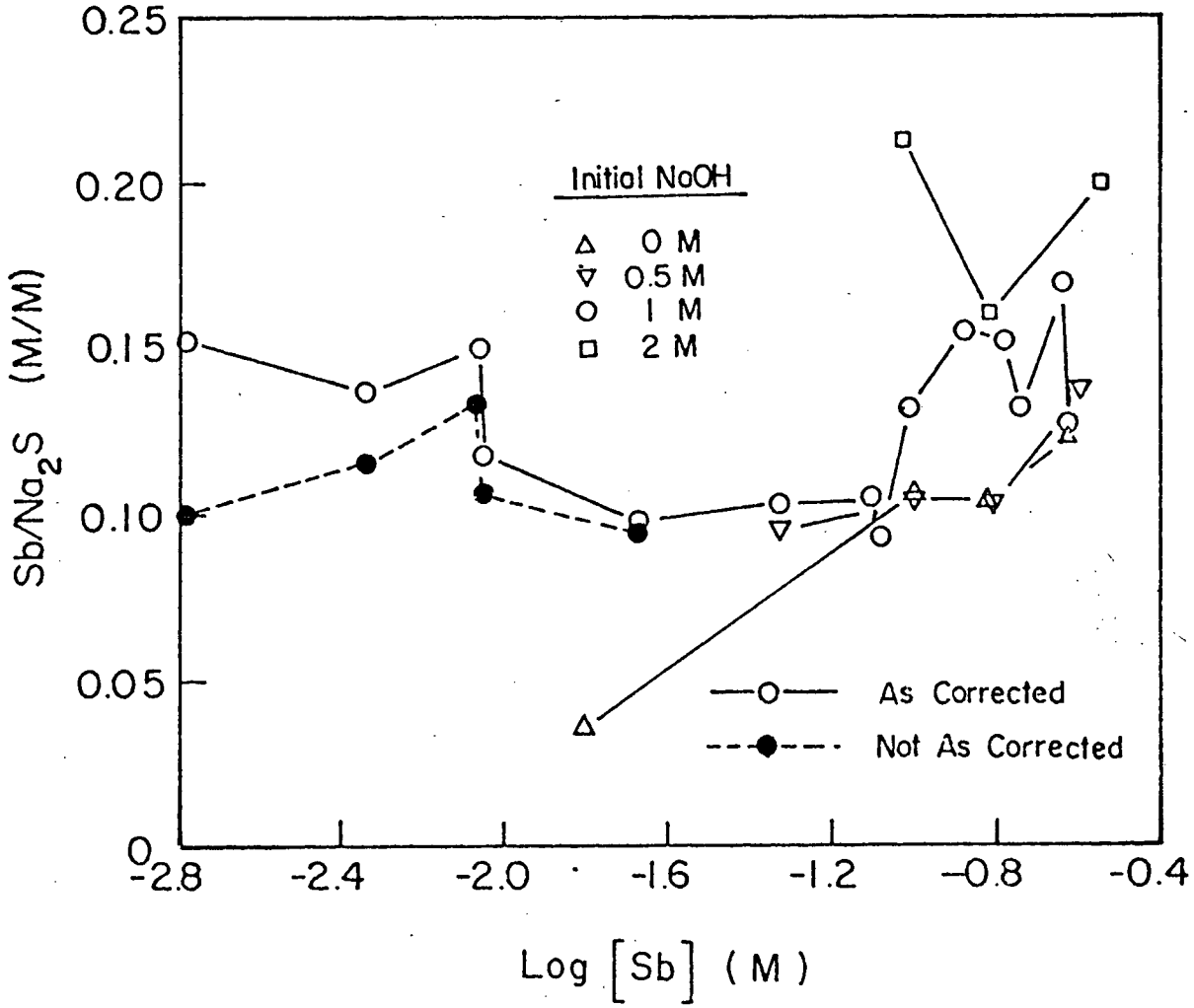

Figure 5-5 The Antimony to Sulphide (Arsenic Corrected) Values versus Log Antimony

If Figures 5-1 and 5-3 are compared (though they are at different temperatures) the discontinuity in Figure 5-3 falls on the experimentally determined border of the SbS_3^{3-} region in Figure 5-1. This acts as a weak piece of evidence for SbS_3^{3-} as the leached antimony species.

Chapter 6.

Discussion

6.1 Review Of The Results

The following results are of significance in understanding the processes occurring during the leach.

i) Antimony was extracted from the concentrate and held in solution. The quantity leached depended on the sodium sulphide and, to a lesser extent, on the sodium hydroxide concentration (Section 4.2.1).

ii) The antomony dissolution results for 1 M initial caustic plotted against the sodium sulphide concentrations were smoothed by addition of a sodium hydroxide factor (Section 4.7).

iii) The net sodium sulphide concentration changes over the 24 hour equilibrium leaching experiments were small. Most of the changes were negative (Section 4.6). However, within the duration of experiments the sodium sulphide levels were observed to both fall and rise.

iv) The net caustic concentration rose in all experiments except in these with sulphide concentrations of greater than 1 M

without added caustic (Section 4.7).

v) An increased concentration of iron was found in the concentrate decomposition product relative to the tetrahedrite phase. The product contained zinc and silver from the tetrahedrite, and manganese, silicon and sodium from solution and from the other phases present in the concentrate (Section 4.13).

vi) Sodium thioferrate appeared to be present in the leached solids (Section 4.3). Sodium, presumably from thioferrate, was extracted by water washing (Section 4.16).

vii) Pyrite was dissolved by sodium sulphide solution and sodium thioferrate was observed to form (Section 4.17).

viii) The concentrate decomposition product was very fine and x-ray amorphous. For these reasons a positive identification of this product was not possible by x-ray diffraction or by microprobe analysis.

6.2 Caustic Formation And Sulphide Depletion

The presence of oxide (and possibly oxidized phases) was confirmed by direct observation and acid leaching (Section4.18 and 2.1.1). If these oxides were to dissolve in caustic and if corresponding sulphides were more stable, then an increase in caustic concentration would occur coupled to a decrease in sulphide (Equations 6-1 and 6-2).

$$MO + 2OH^- = MO_2^{2-} + H_2O \qquad ...(6\text{-}1)$$

$$MO_2^{2-} + S^{2-} + 2H_2O = MS + 4OH^- \qquad ...(6\text{-}2)$$

These changes were observed in the majority of the equilibrium leaching experiments. Fe, Cu, Mn and Si have caustic-soluble species; Fe, Cu and Mn have stable sulphides. Since SiS_2 is unstable in contact with aqueous solution, the possibility of silicon forming a mixed sulphide seems remote.

In the caustic-only leaching experiments no NaOH concentration increase was observed consistent with the proposed mechanism (Section 4.2.2) as no sulphide was present.

In the sulphide-only experiments (Section 4.7) a caustic increase was observed only at low $\{Na_2S\}$ where hydrolysis provided the necessary caustic (Section 1.3.1). The caustic depletion at high $\{Na_2S\}$ was most likely due to the retention of caustic as sodium silicate in the solids.

6.3 Sodium Thioferrate

The inferred presence of sodium thioferrate was ubiquitous to this leaching study. The dispersed colloid was observed in weak sulphide caustic-free solutions (Section 4.3). The leach product contained more sodium than explicable on the basis of entrained leach solution (Section 4.14) and sodium was extractable from these solids by water washing (Section 4.16). Also during washing the filtering rates dropped and there were small breakthroughs of iron-containing material (Section 4.5). This behaviour can be interpreted as the deflocculation of thioferrate mobilizing the sodium and clogging the channels of the filter cake.

Sodium thioferrate, a ferric iron compound, could conceivably be derived from two sources in the concentrate: ferric oxides and pyrite. 10% of the total iron was acid extractable (Section 2.1.1) and the alkaline sulphide dissolution of this iron could produce thioferrate. Thioferrate was shown to be produced by a Na_2S leach on crushed pyrite (Section 4.17) . An internal redox reaction (Equation 6-3)may occur.

$$2FeS_2 + Na_2S + S^{2-} = 2NaFeS_2 + S_2^{2-} \qquad ...(6\text{-}3)$$

This reaction is speculative and has never been previously reported.

The literature indicates that thioferrate should not be stable with respect to decomposition at 100°C (Equation 6-4) (Section 1.3.3).

$$2NaFeS_2 = 2Na^+ + 2Fe^{2+} + S_2^{2-} + 2S^{2-} \quad ...(6\text{-}4)$$

However, sodium (presumably thioferrate sodium) was found in the solids of the 100 and 200°C leaching experiments of Section 4.14 and thioferrate was produced from pyrite at 100°C.

Equation 6-3 provides another mechanism for sulphide depletion. The polysulphide formed could disproportionate since the species is unstable in alkaline solution (Equation 6-7) or, more likely, react with a solid phase(s) present.

$$4S_2^{2-} + 8OH^- = 7S^{2-} + SO_4^{2-} \quad ...(6\text{-}5)$$

6.4 Disintegration Of The Solids

The concentrate was quite fine, more than 50% -400 mesh and crystalline. The leach product, on the other hand, did not appear crystalline at 21,000x and was even finer. The lack of decomposition product diffraction line broadening (as no product diffraction lines were produced) indicated a low crystal order (less than 0.01 μm). Particles of this size are colloidal.

SEM x-ray analyses were done on a number of product areas of a mounted, polished sample of leached solids at 80,000x using a reduced field of observation. Each area showed a spectrum similar to Figure 4-11. The consistent results over many areas at high magnification suggest that the decomposition product is fine and well mixed. Manganese and silicon were found everywhere though their sources are not in the tetrahedrite (Section 4.18). Sodium was not found everywhere, but this may

be an error (Section 4.13).

Because of the indicated fine particle size of the decomposition product and its x-ray amorphous nature, identification of the material by x-ray diffraction or electron microprobe analysis was not possible. For the same reasons it is not certain whether the decomposition product has a definite compostion at all. The product may be a mixture of binary sulphides or a collection of more complex compounds. There is a possibility that the decomposition product includes compounds containing Na_2S (similar to colloidal $NaFeS_2$). This would explain the lack of sulphide in solution in the caustic-only experiments (Section 4.2.3).

6.5 The Characteristics Of The Leach

At low sodium sulphide concentration (Figure 5-2) there appears to be a clear correlation between the antimony and sulphide concentrations as would be expected for an equilibrium between the two. However, at high sulphide concentration where most of the data were collected, there was a great deal of scatter and definitive statements are difficult to make.

In general at high $\{Na_2S\}$ the antimony in solution increased with both sulphide and caustic concentrations. The effect of caustic may be to increase the activity of sulphide relative to the antimony complex, but this does not explain the lack of difference between the 0.5 M and caustic free results

over the same sodium sulphide concentration range (Section 4.2.1). More reasonably, the caustic makes a chemical contribution to the leaching chemistry, a result which seems to be verified by the dependence of the antimony leached on both caustic and sulphide in the 1 M initial caustic experiments (Section 4.7). If the conversion of oxides to sulphides is a source of caustic then the dissolution of antimony may also be associated with this conversion.

Leaching appears to be sensitive to the path that the reactions follow. The two duplicates of Section 4.14 were carefully matched, yet one product solution was 20% higher in antimony than the other. Small differences in mixing or during the short heat-up and initiation period of the leaching tests may have been responsible. Figure 4-8 indicates that the initial antimony dissolution rate can be high - leach 3 was more than one-half complete after 30 minutes when the first sample was taken.

6.6 Sulphide As The Leaching Agent

If tetrahedrite leached in a manner analogous to that of stibnite (Equation 6-6) there would be an equilibrium established between the mineral, sulphide and the antimony complex.

$$Cu_{12}Sb_4S_{13} + S^{2-} = Sb_4S_7^{2-} + 5Cu_2S + CuS \quad ...(6\text{-}6)$$

(In all the leaching reactions written, the antimony complex and leach products written serve only to illustrate the equation rather than describe the actual species. The specific complex formed is unknown and the solid leach product is not likely to be a discreet compound(s) (Section 6.4)). Despite the other reactions occurring in the leach flask, oxide-to- sulphide conversions and thioferrate production, Equation 6-11 would equilibrate reliably given the long experimental duration relative to the apparently fast leaching rates (Section 4.10). The results discussed in the previous section suggest that there is a more complex process which leads to antimony dissolution.

6.7 Thioferrate As The Leaching Agent

The major pieces of evidence that suggest that thioferrate is the leaching agent are its presence in the leach and the increased iron content of the concentrate decomposition product relative to the tetrahedrite.

A thioferrate-tetrahedrite leach can be seen as operating by one of two mechanisms. In the first the $(FeS_2)_n$ chains of thioferrate would come into contact with the tetrahedrite and the iron would react displacing an antimony, or a section of $(FeS_2)_n$ chain would displace an entire SbS_3 group (Equation 6-7).

$$Cu_{12}Sb_4S_{13} + 4NaFeS_2 = 4Na^+ + 2Sb_2S_4^{2-} + Cu_{12}Fe_4S_{13} \quad ...(6\text{-}7)$$

The process is a solid-colloidal reaction which seems difficult. It would be favoured by thermal and shear forces which would shorten the thioferrate chains. Iron replacement for antimony seems more reasonble than extraction of an SbS_3 group as all the SbS sulphurs are bound to non-leaching elements.

By the second mechanism ferrous iron in equilibrium with the thioferrate would be the active agent (Equations 6-8 and 6-9).

$$2NaFeS_2 = 2Na^+ + 2Fe^{2+} + S_2^{2-} + 2S^{2-} \quad ...(6\text{-}8)$$

$$Cu_{12}Sb_4S_{13} + 6Fe^{2+} + 8S^{2-} = 2Sb_2S_4^{2-} + Cu_{12}Fe_4S_{13} \quad ...(6\text{-}9)$$

The process is a solid-solute reaction which would be favoured

by conditions that decompose thioferrate. One of these was given to be temperatures above 80°C (Section 1.3.3).

Both mechanisms presented leach sulphur to maintain the solution charge balance. The sulphur could originate in the pyrite (Mechanism 1, Option 1 and Mechanism 2) or in the tetrahedrite (Mechanism 1, Option 2).

The microprobe analysis indicated that one iron and one sulphur were added to the leach product for each antimony extracted (Section 4.13). Leaching Mechanism 1 has this Fe-Sb stoichiometry while Mechanism 2 would add 1.5 iron atoms per antimony atom extracted. Neither of the two mechanisms postulated adds sulphur to the product. The most likely source of this sulphur is polysulphide formed during thioferrate prouduction.

The pure mixing of thioferrate into the decomposition product would tend to raise the ratio of added iron to added sulphur to 1:2. However, the error inherent in the microprobe analysis of the product (Section 4.13) takes significance away from the microprobe results in general.

6.8 Sodium As The Leaching Agent

Since the changes in sulphide concentration during the leach were relatively small, sodium can be hypothesised as a possible leaching agent (Equation 6-10).

$$Cu_{12}Sb_4S_{13} + 12Na^+ + 8S^{2-} = S_{12}Cu_{12}S_{13} + 2SbS_4^{2-} \quad ...(6\text{-}10)$$

However, the product was found to contain too little sodium; only one sodium per antimony was added versus the expected three (Section 4.14).

6.9 The Leach Equilibrium

Of the three alternatives possible for the leaching agent, thioferrate seems to be the most likely, though the evidence from the experimental results is not overwhelming. Of the two thioferrate mechanisms presented, the first which hypothesises that the iron from the thioferrate chains displaces antimony from tetrahedrite seems more plausible, but again there is no compelling evidence to support this view.

In any case the nature of the leach equilibrium has to be questioned to examine the validity of the equilibrium experiments done. In considering leaching there are three types of solid-solution reaction morphologies. The simplest is simple dissolution, i.e. the solid phase totally enters solution. Equilibrium is achieved by the approach-to-equilibrium kinetics of this dissolution. In leach precipitation a dissolved

component precipitates and the approach to equilibrium is controlled by the precipitation, as well as the dissolution kinetics. In selective dissolution only a portion of the initial solid dissolves leaving a surface residue which may adhere to the substrate if the molal volume change is less than ± 40%. The kinetics of dissolution in this case are grossly affected by the characteristics of the residue and this affects the approach to equilibrium. Leach-precipitation may resemble selective dissolution if precipitation is rapid.

The proposed thioferrate-tetrahedrite leaching mechanism is a combination of two of the morphologies. With respect to tetrahedrite selective leaching occurs leaving a non-adherent colloidal residue. However, the colloid is most likely flocculated (as demonstrated by its settling characteristic (Section 4.5)) which may cause it to form a coating over the substrate tetrahedrite. With respect to the thioferrate leach-precipation occurs where the iron is extracted and enters the leach product. Of course thioferrate itself is the product of a leach - precipitation process and a colloid which mixes in with the decomposition product.

The situation presented is complex and in view of this complexity it is not certain whether the experimental leach tests reached equilibrium or whether the reactions just stifled as the available tetrahedrite surface area became blinded. Alternatively thioferrate may have become unavailable as a reagent due to dilution by the product.

The term 'equilibrium' evokes the concept of a balance between a forward and a backward reaction. In this case it seems unlikely that if dissolved antimony were to be added to the final 'equilibrium' mixtures that incremental tetrahedrite and thioferrate would be the product. Excess thioferrate appears to be present in the leached solids (by the sodium assay) indicating that the production of thioferrate does not control the leaching of the tetrahedrite. The extent of reaction is controlled by the thioferrate-tetrahedrite reaction.

Though the possibility that the leach achieves a true chemical equilibrium is in question the results support such a possibility. With thioferrate as the leaching agent the $Sb(III):S^{2-}$ ratio solubilized is 1:2. To show a slope of unity on a $\log\{Sb\}-\log\{S^{2-}\}$ dissolution plot (Section 5.2), the antimony complex in solution would have to be SbS_3^{3-} (Equation 6-11).

$$Cu_{12}Sb_4S_{12} + 4NaFeS_2 + 4S^{2-} = 4Na^+ + 4SbS_3^{3-} + Cu_{12}Fe_4Sb_{13} \quad ...(6\text{-}11)$$

As discussed previously (Section 5.2) the discontinuity in the tetrahedrite data falls close to the border of SbS_3^{3-} stability as determined by Shestiko and Demina (1971) (Figures 5-1 and 5-3) though the temperatures considered are different. Most of the tetrahedrite data collected occurs in the SbS_3^{3-} stability field.

6.10 The Progress Of The Leach

Examination of the Sb and, in particular, the Na_2S versus time curves of Section 4.10 indicates the leach has two phases. In each phase the conversion of oxides to sulphide and thioferrate production deplete the sulphide concentration and then the tetrahedrite leaching 'catches up' raising the sulphide concentration. The antimony concentration always rises.

The concentrate has a large fraction of fines which have a relatively high surface area (and reactivity). The fines react immediately giving the first phase. Coarser material reacts slower to give the second.

The caustic concentrations were not measured. If they had been they would have showed a steady rise much like the Sb concentrations.

The observation that most of the net sulphide changes were slightly negative is a result of the extent of the reactions given the excess of concentrate used. Below 50% Sb extraction sulphide consuming reactions dominated. Above 50% net increases were observed.

Chapter 7.

Conclusions

An experimental technique was developed to investigate the leaching of tetrahedrite concentrate in sodium sulphide-sodium hydroxide solutions. Analytical chemistry procedures were adapted for the determination of sulphur species, caustic, antimony, and arsenic in the solutions under consideration. X-ray diffraction and electron microscopy were used to study the concentrate and the solid leached product.

From the results the following conclusions can be made :

i) The leaching of antimony does not proceed by the simple extraction of antimony from tetrahedrite leaving solid copper-sulphides.

ii) The leach solutions react, not only with tetrahedrite, but with other phases in the concentrate producing a fine, colloidal, x-ray amorphous residue. Identification of the exact nature of the products in the residue was not possible.

iii) It is unlikely that the solutions produced after 24 hours of leaching represent a true chemical equilibrium. The leaching reaction(s) appears to be hindered by the colloidal character of thioferrate and the decomposition present.

iv) Sulphur is solubilized along with the tetrahedrite antimony. In the range of pulp densities investigated, sulphide depleting reactions kept the net sulphide concentration changes small.

v) Caustic is directly involved in the chemical reactions which lead to antimony dissolution.

vi) The treatment of pyrite with a weak sodium sulphide solution produces sodium thioferrate.

vii) In the leaching of tetrahedrite concentrate the production of thioferrate makes a contribution to the overall caustic-sulphide chemistry. The designation of thioferrate as the tetrahedrite leaching agent could not be made conclusively.

Though many interesting and unexpected results were obtained in this study the work failed to meet its objectives. The leaching experiments did not acheive an unambiguous equilibrium condition and both the solid decomposition product and the antimony complex formed were not identified. The concentrate contained several reactive phases engaging in interlocking reactions. The firm conclusions produced are sparse, though much speculation is possible.

The results produced have a limited application to the Sunshine leaching process. As stated in the introduction the leaching solutions at the Sunshine plant contain oxidized sulphur species which were not added to the experimental leaching mixtures. The sodium sulphide concentrations of the

Sunshine leach solution are higher than those studied in this work and the extractions are higher. The chemical features experimentally observed should be industrially applicable, but they were not well quantified.

The analysis of the literature stibnite solubility data showed that below log{Sb} = -0.7 , $Sb_4S_7^{2-}$ is probably the predominant antimony(III)-sulphide complex in saturated solution at 25°C. Above log{Sb} = -0.7 , $Sb_4S_7^{2-}$ is the most likely predominant complex. The complexes SbS_2^-, SbS_3^{3-} and $Sb_2S_5^{4-}$ are minor species in stibnite-saturated solutions.

Chapter 8.

Recommendations for Future Study

Much further work is warranted in the study of the alkaline sulphide leaching of tetrahedrite. The following is a summary of recommendations.

i) prepare "pure" tetrahedrite and investigate the effect of sulphide and thioferrate on this material

ii) investigate the production of thioferrate from pyrite by sulphide, both chemically and electrochemically

iii) investigate the effect of oxidized sulphur species on antimony extraction and the other phases present in the tetrahedrite concentrate

Appendix A: The $HS^- - S^{2-} - OH^-$ Equilibrium Calculation at 100°C

The data was taken from Ferreira (1975). No activity coefficient data was available for HS^- and S^{2-} to make corrections.

$$H_2O = H^+ + OH^- \qquad \ldots(A\text{-}1)$$

$$K_1 = \{H^+\}\{OH^-\} = 10^{-12.21}$$

$$H^+ + S^{2-} = HS^- \qquad \ldots(A\text{-}2)$$

$$K_2 = \frac{\{HS^-\}}{\{H^+\}\{S^{2-}\}} = 10^{10.98}$$

$$K_1 K_2 = \frac{\{OH^-\}\{HS^-\}}{\{S^{2-}\}} = 10^{-1.23} = 0.0589$$

$$zOH^- + yS^{2-} + xH_2O = xHS^- + (y-x)S^{2-} + (z+x)OH^-$$

$$\frac{(z+x)(x)}{y-x} = 0.0589$$

$$x = \frac{-(z + 0.058) + \sqrt{(z + 0.058)^2 + 0.2355y}}{2}$$

$$\text{Fraction added } Na_2S \text{ as } S^{2-} = \frac{y-x}{y}$$

Appendix B: X-ray Diffractometry

Table B-1: X-Ray Diffractometry Results*

Measured 2θ(deg)	d (Å)	RI (%)	Assignment**	hkl	Lit d. (Å)
11.99	7.38	5	AT	011	7.3
16.90	5.24	5	T	002	5.2
24.08	3.69	15	T	022	3.69
25.95	3.43	5	M/G	110/111	3.44/3.43
29.62	3.01	100	AT/T//C	222//112	3.00//3.03
31.99	2.79	15	AT	123	2.80
33.02	2.71	20	M/P	020/200	2.71/2.71
34.26	2.61	15	T	004	2.61
36.50	2.56	10			
36.95	2.43	5	T/P	003210	2.46/2.42
38.48	2.34	5			
40.73	2.21	5	P	211	2.212
43.10	2.10	5	G	220	2.099
44.25	2.05	5	T	015,134	2.04
44.72	2.03	5			
44.70	1.91	5			

Table B-1: X-ray Diffractometry Results* (cont)

Measured 2_θ(deg)	d (Å)	RI (%)	Assignment**	hkl	Lit. d (Å)
4905	1.91	15	C	024	1.854
49.49	1.86	25	AT	044	1.855
51.06	1.79	5	M	211	1.76
54.03	1.70	5	T	116,234	1.687
56.25	1.63	5	T/P	026/311	1.65/1.63
57.75	1.60	5	C	132	1.59
58.65	1.57	10	AT	226	1.58
65.05	1.43	5			

* spectrum taken at 40 KV and 20 mA, Cu Kα radiation

**Assignment Legend

		ASTM File #
AT	Argentian Tetrahedrite	11-101
C	Chalcopyrite	9-423
G	Galena	5-0592
M	Marcasite	3-0799
P	Pyrite	6-0710
T	Tetrahedrite	11-107

Appendix C: Concentrate Stoichiometry Calculations

Calculation was based on 100 g of dry concentrate with the composition given in the table below. Mn was not considered.

Element	%	MW (g/mol)	Moles
Cu	26.0	63.55	0.409
Fe	14.6	55.85	0.261
Sb	13.1	121.75	0.108
S	29.1	32.06	0.908
As	1.58	74.92	0.021
Zn	1.67	65.38	0.026
Ag	3.6	107.87	0.033

Assuming all the arsenic and antimony are contained in the tetrahedrite. The Sb + As:S ratio is 4:13 so S must be 0.419 moles. Also Sb+As:Ag+Zn+Cu+Fe is 4:12 so Cu+Fe is 0.328 moles. Assuming that the only other Fe, Cu and S containing phases are $CuFeS_2$ and FeS_2 the distribution of these elements was calculated.

Let:

x = Cu in tetrahedrite

y = Fe in tetrahedrite

a = relative moles of $CuFeS_2$

b = relative moles of FeS_2

Equations:

$$x + y = 0.328$$

$$a = 0.409 - x$$

$$b = 0.261 - a - y$$

$$2a + 2b = (0.908 - 0.419)$$

Solving:

$$x = 0.3115$$

$$y = 0.0165$$

$$a = 0.0975$$

$$b = 0.147$$

Result: $(Cu_{9.7}, Fe_{0.5})(Ag_{1.0}Zn_{0.8})(Sb_{3.4}As_{0.6})S_{13} +$

$$3.0\ CuFeS_2 + 4.6\ FeS_2$$

Lead was the only sulphide mineral element not determined. Since it would tie up extra sulphur as galena, 2a + 2b would be smaller and the Fe:Cu ratio of the tetrahedrite would rise. For example, if the concentrate were 3% lead the analysis would yield:

$(Cu_{9.4}Fe_{0.7}Zn_{0.8}Ag_{1.0})(Sb_{3.4}As_{0.6})S_{13} + 0.4\ PbS +$

$$3.2\ CuFeS_2 + 4.1\ FeS_2$$

A lead content as high as 3% is unlikely.

Appendix D: Experimental Results

Table D-1: Data for Leaching Experiments Considered in the Study

Final Solution Analysis									Initial Conditions				
Sb (g/l	OH^- (M)	S^{2-} (M)	$S_2O_3^{2-}$ (M)	SO_3^{2-} (M)	S^o (M)	$*S^{2-}$ (M)	As (g/l)	Extraction (%)	S^{2-} (M)	OH^- (M)	Leach Vol (ml)	Conc (g-wet)	Conc. H_2O (%)
0.202	(1.03)	0.0168						1	0.0278	(1.03)	130	25	7.24
0.556	(1.03)	0.0398						2	0.0593	↓	↓	↓	↓
1.07	(1.03)	0.0659						5	0.0943				
1.08	(1.03)	0.0834						5	0.124				
2.63	1.06	0.230	-	0.01	-	0.01	0.38	11	0.265	(0.99)			7.50
5.75	1.11	0.48	-	0.07	-	0.01		22	0.48	↓			↓
9.58	1.23	0.77	*	*	*	0.03		41	0.79				
10.2	1.12	0.93	*	*	*	0.02		44	0.96				
11.9	1.22	0.780	-	-	-	0.04	1.13	26	0.793			50	
16.1	1.24	0.901	0.05	0.01	0.01	0.03	1.36	35	0.947			↓	
21.2	1.27	1.18	0.03	*	0.07	0.07		46	1.26				
22.2	1.21	1.44	0.12	*	*	0.02		48	1.46				
28.0	1.30	1.42	*	*	*	0.06	2.18	42	1.48			75	
28.9	1.04	1.86	*	*	*	0.06		62	1.73	↓	↓	50	↓

Table D-1: Data for Leaching Experiments Considered in the Study (cont)

Final Solution Analysis								Extraction from solids	Initial Conditions				
Sb (g/l)	OH- (M)	S^{2-} (M)	$S_2O_3^{2-}$ (M)	SO_3^{2-} (M)	S^o (M)	$*S^{2-}$ (M)	As (g/l)	(%)	S^{2-} (M)	OH- (M)	Leach vol (ml)	Conc. (g-wet)	Conc. H_2O (%)
11.5	2.19	0.470	-	0.04	0.02	0.03		25	0.505	(1.98)	130	50	7.50
18.5	2.12	1.01	-	0.05	0.04	0.03		40	1.02	↓	↓	50	↓
34.0	2.17	1.46						49	1.54			75	
5.75	0.62	0.510	-	-	-	0.01	0.53	12	0.55	(0.50)	130	25	7.50
12.2	0.64	0.987	-	-	-	0.02	1.08	26	1.06	↓	↓	50	↓
18.8	0.69	1.54	-	-	-	0.03	1.25	40	1.50			50	
31.2	0.82	1.92	0.02	*	0.03	0.02	2.25	45	1.99			75	
1.90.	0.15	0.446	0.03	0.01	-		0.29	8	0.587	(-)	130	25	7.50
12.3	0.05	0.979	-		0.04	0.09	1.13	24	1.08	↓	↓	50	↓
18.4	-0.02	1.49	0.02	0.01	-	*	1.48	40	1.52			50	
28.4	-0.09	1.96	0.06	0.04		0.04	2.13	41	2.10			75	
0.33	[0.45]	-						1	(-)	0.52	130	25	7.42
0.54	[0.96]	-						2	↓	1.03	↓	25	↓
0.35	[2.08]	-						1		2.08		25	

Legend:
- ( ) indicates value calculated
- [ ] value equivalent to 2nd end point (Section 4.2.2)
- - value of zero determined
- * result impossible to interpret
- $*S^{2-}$ difference between normal $[S^{2-}]$ determination and $[S^{2-}]$ determination after Na_2SO_3 treatment; potential measure of Sb (V)

Table D-2: Data for Leaching Experiments Not Considered

Final Solution Analysis						Initial Conditions			
Sb (g/l)	OH^- (M)	S^{2-} (M)	$S_2O_3^{2-}$ (M)	SO_3^{2-} (M)	S^o (M)	S^{2-} (M)	OH^- (M)	Leach Vol. (ml)	Conc (g-wet)
6.75	1.07	0.42	0.04	-	0.03	0.48	(1.02)	180	50
13.9	1.09	0.85	0.06		-	0.96	(1.01)	200	75
14.1	1.14	0.84	0.10		0.01	0.96	(1.00)	180	75
23.3	1.17	1.33	0.14		-	1.45	(1.00)	200	100
31.3		1.60	-		0.03	1.95	(1.00)	200	125
31.6	1.35	2.32	0.16		0.11	2.45	1.15	140	75
37.3	1.42	1.83	-	0.10	-	1.78	1.14	120	60
46.1	1.20	2.59	-		0.09	2.51	1.17	120	75
49.7	1.25	2.83	-		0.08	2.83	1.04	120	85
17.8	1.17	0.87	0.12		0.02	0.99	(2.00)	200	75
22.9	2.24	0.94	0.10	0.01	0.02	0.97	2.00	120	60
27.3	2.75	1.30	0.16		0.19	1.35	2.25	140	60
38.6	2.22	1.86	-	0.06	0 05	1.92	2.08	120	60
41.7	2.90	1.87	0.22		0.02	1.88	2.92	120	75
44.1	2.64	1.94	0.24		0.02	1.98	2.14	120	75
54.8	5.96	1.57	-	0.09		0.92	3.89	120	60
10.6	1.68	0.43	0.34	0.05		0.32	0.99		
40.7	1.59	2.53	-	0.10		1.94	0.97		
36.2	2.79	2.05				2.07	1.98		

Appendix E: Antimony and Sulphide Concentrations versus Time

All the leaches were started with 170 ml of solution and 75 g of wet concentrate. Leaches 1 and 3 were 1 M initial NaOH; 2 and 4 : 2 M NaOH (calculated, not measured). The leach temperature was 100 C. Each sample was 10 ml.

Table E-1: Sb and Na_2S versus Time Results

	Leach 1		Leach 2	
Time (min)	Sb (g/l)	Na_2S (M)	Sb (g/l)	Na_2S (M)
0	0	0.848	0	0.862
30	3.60	0.627	6.50	0.667
60	5.20	0.595	9.33	0.698
120	7.18	0.660	13.6	0.750
240	10.1	0.663	15.8	0.736
480	14.7	0.701	19.5	0.776
1440	16.3	0.726	20.9	0.781

	Leach 3		Leach 4	
Time (min)	Sb (g/l)	Na_2S (M)	Sb (g/l)	Na_2S (M)
0	0	1.56	0	1.45
30	15.8	1.46	18.6	1.42
60	18.6	1.52	20.3	1.53
120	20.3	1.48	22.3	1.48
240	21.5	1.51	-	-
480	25.0	1.54	27.3	1.52
1440	28.2	1.57	-	-

Appendix F: Analysis of the Stibnite Dissolution Data

The data of Arntson *et al.* (1966) was converted from weight percent Na_2S, Sb_2S_3 and H_2O to concentrations of S and Sb by considering the molarity of these solutions to be equal to their molality. The appropriate number of moles of S^{-2} per mole of Sb were subtracted from the total $\{S^{2-}\}$ for the complex considered and the $HS^- - S^{-2} - OH^-$ equilibrium was calculated to determine the concentration of free S^{-2}. A calculation parallel to that shown in Appendix A was used with the following constants (25°C):

$$K_1 = \{H^+\}\{OH^-\} = 10^{-13.997}$$

$$K_2 = \{HS^-\}/\{H^+\}\{S^{2-}\} = 10^{12.92}$$

$$K_1 K_2 = 0.0838$$

Table F-1: Results of Log (Sb) - Log (Free S^{2-}) Calculations

Data from Arntson et al.				Complex Considered: log [Free S^{2-}] (M)			
Na_2S (mol/kg soln)	Sb_2S_3 (mol/kg soln)	H_2O (%/100)	log[Sb] (M)	$Sb_4S_7^{2-}$	$Sb_2S_4^{2-}$	$Sb_2S_5^{4-}$	SbS_3^{3-}
0.058	0.0138	0.9908	-1.559	-1.809	-1.907	-2.167	-2.612
0.094	0.0250	0.9842	-1.294	-1.502	-1.608	-1,905	-2.505
0.155	0.0426	0.9734	-1.058	-1.193	-1.297	-1.594	-2.234
0.241	0.0683	0.9580	-0.846	-0.932	-1.035	-1.332	-2.023
0.250	0.0712	0.9563	-0.827	-0.911	-1.014	-1.313	-2.016
0.315	0.1080	0.9387	-0.638	-0.791	-0.920	-1.352	-2.837
0.464	0.1667	0.9072	-0.434	-0.570	-0.720	-1.166	-
0.496	0.1766	0.9013	-0.407	-0.530	-0.660	-1.107	-
0.629	0.2325	0.8719	-0.273	-0.393	-0.527	-1.010	-
0.672	0.2576	0.8600	-0.223	-0.357	-0.497	-1.028	-
0.728	0.2682	0.8521	-0.201	-0.307	-0.438	-1.909	-
0.830	0.3285	0.8236	-0.098	-0.232	-0.376	-0.948	-
0.917	0.3694	0.8029	-0.036	-0.171	-0.318	-0.917	-

Table F-2: Results of Equilibrium Constant Calculations

Na_2S (mol/kg soln)	Sb_2S_3 (mol/kg soln)	$K(Sb_4S_7^{2-})$ free S^{2-} basis	$K(Sb_2S_4^{2-})$ free S^{2-} basis
0.058	0.0138	0.444	1.114
0.094	0.0250	0.404	1.030
0.155	0.0426	0.341	0.867
0.241	0.0683	0.305	0.773
0.250	0.0712	0.303	0.946
0.315	0.1080	0.356	0.957
0.464	0.1667	0.341	0.965
0.496	0.1776	0.332	0.895
0.629	0.2325	0.330	0.897
0.672	0.2576	0.340	0.940
0.728	0.2682	0.319	0.863
0.830	0.3285	0.340	0.948
0.917	0.3694	0.341	0.957

Mean $K(Sb_4S_7^{2-})$ last 8 = 0.337±0.008 (95% confidence level)

Mean $K(Sb_2S_4^{2-})$ first 5 = 0.95±0.15

Table F-3: Results from Calculations on Data from Dubey and Ghosh (1962)

Literature Data $Sb_2S_4^{2-}$ formed (M)	Res Na_2S (M)	log Sb (M)	log {free S^{2-}} (M)	$K(Sb_2S_4^{2-})$
0.5 M KCl:				
0.00985	0.02563	-1.706	-2.296	1.949
0.01081	0.02974	-1.665	-2.189	1.672
0.01503	0.03059	-1.522	-2.169	2.219
0.01793	0.03276	-1.445	-2.121	2.367
0.01965	0.03611	-1.406	-2.053	2.217
1 M KCl:				
0.01009	0.02722	-1.695	-2.253	1.806
0.01264	0.03000	-1.597	-2.183	1.927
0.01413	0.03170	-1.549	-2.144	1.968
0.01518	0.03279	-1.518	-2.120	2.001
0.01690	0.03640	-1.471	-2.047	1.882
0.02054	0.03808	-1.386	-2.015	2.130

All Results Mean K = 2.01±0.13 (95% confidence level)

0.5 M KCl: Mean K = 2.08±0.31

1.0 M KCl Mean K = 1.95±0.11

*the complex $Sb_2S_4^{2-}$ was considered

Appendix G: Calculation of Log Antimony and Log Sulphide Data from Experimental Results

The experimental results were converted into log antimony and log sulphide form. Six different forms of log sulphide data were calculated: log {total S^{2-}}, log {free S^{2-}} and log {residual free S^{2-}} considering the complexes - $Sb_4S_7^{2-}$, $Sb_2S_4^{2-}$, $Sb_2S_5^{4-}$ and SbS_3^{3-}. In all cases a correction was made for arsenic as AsS_2^- using the relationship determined in Section 4.8 (Equation G-1).

$$As(M) = 0.110\ Sb(M) + 0.000278 \qquad ...(G\text{-}1)$$

The $HS^- - S^{2-} - OH^-$ equilibrium at 100°C (Appendix A) was calculated to determine the free S^{-2} concentration after the appropriate number of moles of S^{-2} per mole of Sb were deducted for the complex under consideration.

Table G-1: Results of Calculations for Log Antimony versus Log Sulphide Plots

Sb (M)	OH^- (M)	S^{2-} (M)	log [Sb] (M)	log [Total S^{2-}]* (M)	log [Free S^{2-}]* (M)				
					-	$Sb_4S_7^{2-}$	$Sb_2S_4^{2-}$	$Sb_2S_5^{4-}$	SbS_3^{3-}
0.00166	(1.03)	0.0168	-2.780	-1.964	-1.988	-2.123	-2.146	-2.196	-2.254
0.00457	(1.03)	0.0398	-2.340	-1.478	-1.503	-1.622	-1.642	-1.661	-1.734
0.00879	(1.03)	0.0659	-2.056	-1.234	-1.256	-1.390	-1.413	-1.461	-1.518
0.00887	(1.03)	0.0834	-2.052	-1.120	-1.143	-1.243	-1.258	-1.293	-1.331
0.0216	1.06	0.23	-1.666	-0.658	-0.681	-0.763	-0.777	-0.804	-0.833
0.0472	1.11	0.48	-1.326	-0.333	-0.355	-0.441	-0.454	-0.483	-0.514
0.0787	1.23	0.77	-1.104	-0.127	-0.146	-0.235	-0.249	-0.279	-0.312
0.0838	1.12	0.93	-1.077	-0.043	-0.064	-0.141	-0.153	-0.179	-0.206
0.0977	1.22	0.780	-1.010	-0.123	-0.143	-0.255	-0.274	-0.314	-0.358
0.133	1.24	0.901	-0.878	-0.063	-0.082	-0.219	-0.242	-0.293	-0.351
0.174	1.27	1.18	-0.759	0.055	0.036	-0.099	-0.123	-0.173	-0.231
0.182	1.21	1.41	-0.739	0.135	0.115	0.000	-0.020	-0.061	-0.107
0.230	1.30	1.42	-0.638	0.135	0.116	-0.036	-0.063	-0.122	-0.190
0.237	1.04	1.86	-0.625	0.256	0.234	0.120	0.101	0.060	0.015

* sulphide values corrected for arsenic (AsS_2^-)

Table G-1: Results of Calculations for Log Antimony versus Log Sulphide Plots (cont)

Sb (M)	OH^- (M)	S^{2-} (M)	log Sb (M)	log [Total S^{2-}]* (M)	log [Free S^{2-}]*(M)				
					-	$Sb_4S_7^{2-}$	$Sb_2S_4^{2-}$	$Sb_2S_5^{4-}$	SbS_3^{3-}
0.0945	2.19	0.470	-1.025	-0.353	-0.364	-0.567	-0.606	-0.695	-0.807
0.152	2.12	1.01	-0.818	-0.013	0.025	-0.164	-0.188	-0.240	-0.300
0.279	2.17	1.46	-0.554	-0.144	0.133	-0.055	-0.090	-0.169	-0.266
0.0472	0.62	0.510	-1.326	-0.306	-0.343	-0.423	-0.436	-0.462	-0.491
0.0998	0.64	0.99	-1.001	-0.017	-0.049	-0.139	-0.153	-0.182	-0.214
0.154	0.69	1.54	-0.811	0.176	0.145	-0.059	0.045	0.015	-0.016
0.256	0.82	1.92	-0.591	0.269	0.244	0.122	0.102	0.058	-0.010
0.0156	0.15	0.446	-1.807	-0.356	-0.452	-0.481	-0.485	-0.494	-0.503
0.101	0.05	0.979	-0.995	-0.021	-0.117	-0.215	-0.231	-0.264	-0.300
0.151	-0.02	1.49	-0.822	0.162	0.061	-0.039	-0.055	-0.089	-0.126
0.233	-0.09	1.96	-0.632	0.279	0.156	0.027	0.006	-0.041	-0.094

* sulphide values corrected for arsenic (As S_2^-)

Table G-2: Antimony to Sulphide Ratios

Sb (M)	OH^- (M)	S^{2-} (M)	S^{2-} (M) {As Corr}	Sb/S^{2-} {As Corr} (mole/mole)
0.00166	(1.03)	0.0168	0.0109	0.153
0.00457	(1.03)	0.0398	0.0333	0.138
0.00879	(1.03)	0.0659	0.0583	0.151
0.00887	(1.03)	0.0834	0.0759	0.117
0.0216	1.06	0.23	0.22	0.098
0.0472	1.11	0.48	0.46	0.102
0.0787	1.23	0.77	0.75	0.105
0.0838	1.12	0.93	0.91	0.093
0.0977	1.22	0.78	0.75	0.130
0.133	1.24	0.90	0.87	0.154
0.174	1.27	1.18	1.14	0.153
0.182	1.21	1.41	1.36	0.133
0.230	1.30	1.42	1.36	0.169
0.237	1.04	1.86	1.80	0.131

Table G-2: Antimony to Sulphide Ratios (cont.)

Sb (M)	OH^- (M)	S^{2-} (M)	S^{2-} (M) {As Corr}	Sb/S^{2-} {As Corr} (mole/mole)
0.0945	2.19	0.470	0.44	0.213
0.152	2.12	1.01	0.97	0.157
0.279	2.17	1.46	1.39	0.200
0.0472	0.62	0.510	0.49	0.095
0.0998	0.64	0.99	0.96	0.104
0.154	0.69	1.54	1.50	0.103
0.256	0.82	1.92	1.86	0.138
0.0156	0.15	0.446	0.44	0.035
0.101	0.05	0.979	0.95	0.106
0.151	-0.02	1.49	1.45	0.104
0.233	-0.09	1.96	1.90	0.123

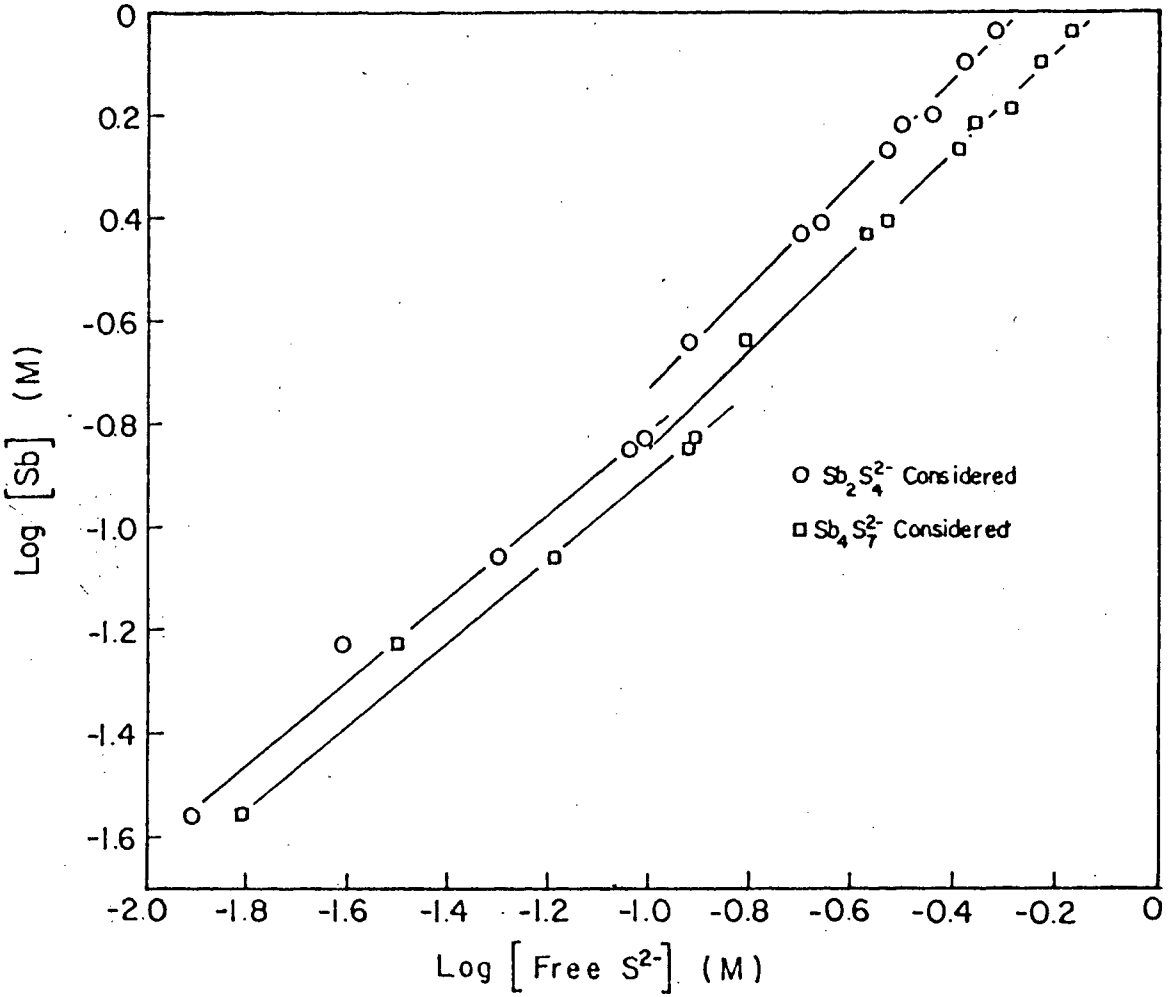

Figure G-1 The Stibnite Solubility Data of Arntson et al. (1966) Plotted Considering $Sb_2S_4^{2-}$ and $Sb_4S_7^{2-}$

REFERENCES

Arntson, R.H., F.W. Dickson and G. Tunell. Science (1966) 153 , p. 1673.

Baiborov, P.P., A.P. Ezhkov and S. Ishankhodzhaev. Khim. Redk. Tsvetn. Met. (1975). pp. 71-109.

Baiborov, P.P. Tsvetn. Met. (1975). pp.25-27.

Barner, H.E. And R.V. Scheuerman. Handbook of Thermochemical Data for Compound and Aqueous Species (New York, 1978). John Wiley & Sons.

Barr, L.N. Sunshine Mining Co.-Metallurgy Summary (Sunshine, Idaho, 1973), Sunshine Mining Co.

Bassett, J., R.C. Denney, G.H. Jeffery and J. Mendham. Vogel's Textbook of Quantitative Inorganic Analysis , (London, 1978), Longman.

Blasius, E., G. Horn, A. Knochel, J. Munch and H. Wagner. Inorganic Sulphur Chemistry , G. Nickless (ed.), (Amsterdam, 1968), Elseveir Publishing Co., pp. 199-239.

Buslaev, Y.A., E.A. Krauchenko, I.A. Kuz'min, V.B. Lazarev, and A.B. Salov. Russian J. Inorg. Chem. (1971) 6 , pp. 1782-1784.

Butler, J.N. Ionic Equilibrium: A Mathematical Approach . (Reading, Massachusetts, 1964), Addison Wesley Publishing Co.

Dubey, K.P., and S. Ghosh. Z. Anorg. Allg Chem. (1962) 31 , pp. 204-207.

Ferreira, R.C.H. Leaching and Reduction in Hydrometallurgy, A.R. Burkin (ed.),(London, 1975), IMM, pp. 67-83.

Homes, W.C. EMJ (1944), 145 , pp. 54-58.

Latimer, W.E. The Oxidation States of the Elements and Their Potentials in Aqueous Solutions (2nd. Ed.),(Englewood Cliffs, New Jersey, 1952), Prentice Hall Inc.

Moss, K.C. And M.A.R. Smith. Inorganic Chemistry: Series Two. Vol. 2: Main Group Element Groups IV and V , D.B. Sowerby (ed.),(London, 1975), Butterworths pp. 221-267.

Papp, J. Cell. Chem. Tech. (1971) 5 , pp. 147-159.

Scavnicar, S. Z. Kristallogr. (1960), 114 ,pp. 85-97.

Seuryukov, M.N. and R. Murti. Zavod. Lab., 32 , pp. 144-146.

Shestiko, V.S. and O.P. Demina. Zh. Neorg. Khim. (1971), 16 p. 3167.

Sillen, L.G. and A.E. Martell. Stability Constants of Metal-Ion Complexes ,(London, 1964), The Chemical Society.

Takeuchi, Y. And R. Sadanga. Z. Kristallogr. (1969) 130 , pp. 346-368.

Tatsuka, K. and N. Morimoto. Am. Mineral. (1973), 58, pp. 425-434.

Taylor, P. And D.W. Shoesmith. Can. J. Chem. (1978), 22 , pp. 2798-2802.

Vaugham, D.J. And J.R. Craig. Mineral Chemistry of Metal Sulphides,(London, 1978), Cambridge University Press.

Wuensch, B.J. Z. Kristallogr., 1964, 11 ,pp. 437-453.